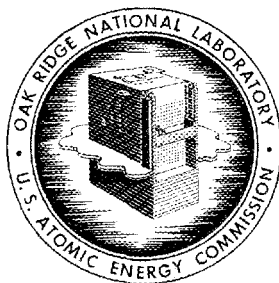


ORNL
MASTER COPY

11



OAK RIDGE NATIONAL LABORATORY

operated by

UNION CARBIDE CORPORATION

NUCLEAR DIVISION

for the

U.S. ATOMIC ENERGY COMMISSION



ORNL - TM - 1780

PREPARATION OF POROUS THORIA BY INCORPORATION
OF CARBON IN SOLS

NOTICE This document contains information of a preliminary nature and was prepared primarily for internal use at the Oak Ridge National Laboratory. It is subject to revision or correction and therefore does not represent a final report.

LEGAL NOTICE

This report was prepared as an account of Government sponsored work. Neither the United States, nor the Commission, nor any person acting on behalf of the Commission:

- A. Makes any warranty or representation, expressed or implied, with respect to the accuracy, completeness, or usefulness of the information contained in this report, or that the use of any information, apparatus, method, or process disclosed in this report may not infringe privately owned rights; or
- B. Assumes any liabilities with respect to the use of, or for damages resulting from the use of any information, apparatus, method, or process disclosed in this report.

As used in the above, "person acting on behalf of the Commission" includes any employee or contractor of the Commission, or employee of such contractor, to the extent that such employee or contractor of the Commission, or employee of such contractor prepares, disseminates, or provides access to, any information pursuant to his employment or contract with the Commission, or his employment with such contractor.

ORNL-TM-1780

Contract No. W-7405-eng-26

CHEMICAL TECHNOLOGY DIVISION

PREPARATION OF POROUS THORIA BY INCORPORATION
OF CARBON IN SOLS

K. J. Notz

DECEMBER 1968

OAK RIDGE NATIONAL LABORATORY
Oak Ridge, Tennessee
operated by
UNION CARBIDE CORPORATION
for the
U. S. ATOMIC ENERGY COMMISSION

CONTENTS

	<u>Page</u>
Abstract	1
1. Introduction	1
2. Experimental	1
2.1 Materials	1
2.1.1 Thoria Sol	3
2.1.2 Carbon	5
2.2 Preparation of Sols and Gels	5
2.2.1 Preparation of Sols	5
2.2.2 Preparation of Gels	11
2.2.3 Firing and Carbon Burnout	13
2.3 Analytical Methods	14
3. Results and Discussion	15
3.1 Major Variables: C/ThO ₂ Mole Ratio and Carbon Burnout Procedure	15
3.2 Minor Variables and Reproducibility	19
3.3 Other Factors Related to Firing Schedule	24
3.3.1 Variations in Firing Cycle	24
3.3.2 Thermal Stability of Product	25
3.4 General Structure	28
3.4.1 Density, Pore Size Distribution, and Hardness	28
3.4.2 Surface Area and Structure	32
3.5 Residual Carbon	40
3.6 Graphite as Carbon Source	41
3.7 Porous Microspheres	43
3.8 Kinetics of Carbon Burnout	47
3.9 Porous (Th,U)O ₂	50
4. Summary and Conclusions	52
5. Acknowledgements	54
6. References	55

PREPARATION OF POROUS THORIA BY INCORPORATION
OF CARBON IN SOLS

K. J. Notz

ABSTRACT

Porous thoria with a wide range of controlled porosity was prepared by a sol-gel technique. Carbon was incorporated in thoria sols to produce stable mixed sols, which were gelled as either shards or microspheres. Subsequent removal of the carbon by combustion in air under appropriate conditions yielded thoria with porosities ranging from less than 1 to 72%. The two major variables affecting porosity are the C/ThO₂ mole ratio and the firing schedule. When the thoria matrix is first "set" by sintering at a high temperature and the carbon is then burned out at a lower temperature, the resultant porosity is approximately equal to the calculated volume of the removed carbon. After carbon removal, subsequent exposure to high temperatures sinters out much of the introduced porosity. In some cases, pore size distributions over narrow ranges are obtained in the submicron range. The pore size varies with both the carbon content and with the firing procedure; it can also be altered by using different sources of carbon. Surface area and density data, in conjunction with porosity values, were used to construct a realistic interpretation of the gelation and the sintering mechanisms. The kinetics of carbon burnout was studied, and an activation energy of 41 kcal/mole was determined for burning in air at 440 to 500°C. Carbon removal with steam, CO₂, and hydrogen was examined briefly. Porous (Th,U)O₂ was also prepared by the same method used for porous ThO₂.

1. INTRODUCTION

For nuclear fuel applications, the incorporation of a controlled amount of porosity in thoria is of interest for the following reasons: (1) to relieve pressure buildup due to evolved gases in encapsulated fuels, (2) to provide an escape path for gaseous fission products in vented fuels, (3) to limit and control fuel density, (4) to provide a relief for thermal and radiation-induced stresses, (5) to increase dissolution rates during fuel

reprocessing, and (6) to permit the addition of a second phase within the oxide matrix where this may be desirable or necessary. From a more general viewpoint, an inorganic oxide with a narrow pore size distribution in the <100- to 1000-Å range is potentially useful as a chromatographic medium for biological separations,¹ or as a substrate for hyperfiltration membranes and related applications.²

Methods for fabricating fuels by the sol-gel process are receiving attention because of the advantages inherent in this process. It has previously been demonstrated at ORNL that a low level of porosity (up to 5%) can be introduced in (Th,U)O₂ by adding lampblack to the sol and then burning the carbon out of the resulting gel.³ Porous (Th,U)O₂ was prepared for the Dragon project using the same general method, but details of that work are not available; it has been reported that porosities in the 10 to 60% range were obtained.^{4,5} Another method involves incorporation and subsequent volatilization of MoO₃; this method has been demonstrated over the porosity range 20 to 33%.⁶ Urania with porosities of 1 to 44% has been made from chloride-base sols by leaving residual chloride in the gel and subsequently driving it off as HCl.⁶

Experience gained previously in the preparation of ThO₂-carbon black sols showed that mixed sols of exceptional stability can be obtained over a composition range from zero to as high as 15 moles of carbon per mole of ThO₂.⁷ Preliminary experiments in which carbon black was burned out of C-ThO₂ gels yielded two interesting products: one with a porosity of 37%, in the 220- to 350-Å range; and the other with a porosity of 58%, all pores having a diameter of less than 120 Å.⁸

The primary objectives of the present program were to prepare porous thoria by a sol-gel technique and to determine the effects of the two major variables, the C/ThO₂ mole ratio and the carbon burnout procedure, on porosity and pore size distribution. In addition, a number of other factors were also studied: type of carbon used, variations in sol preparation and gelation technique, and the type of product formed (shards vs microspheres). The kinetics of carbon burnout were examined briefly. A porous mixed oxide of composition Th_{0.78}U_{0.22}O₂ was prepared for comparison with ThO₂.

This report includes work conducted in cooperation with the MIT School of Chemical Engineering Practice. That portion of the work was conducted by A. H. Mesch and C. K. Neulander.⁹

2. EXPERIMENTAL

2.1 Materials

2.1.1 Thoria Sol

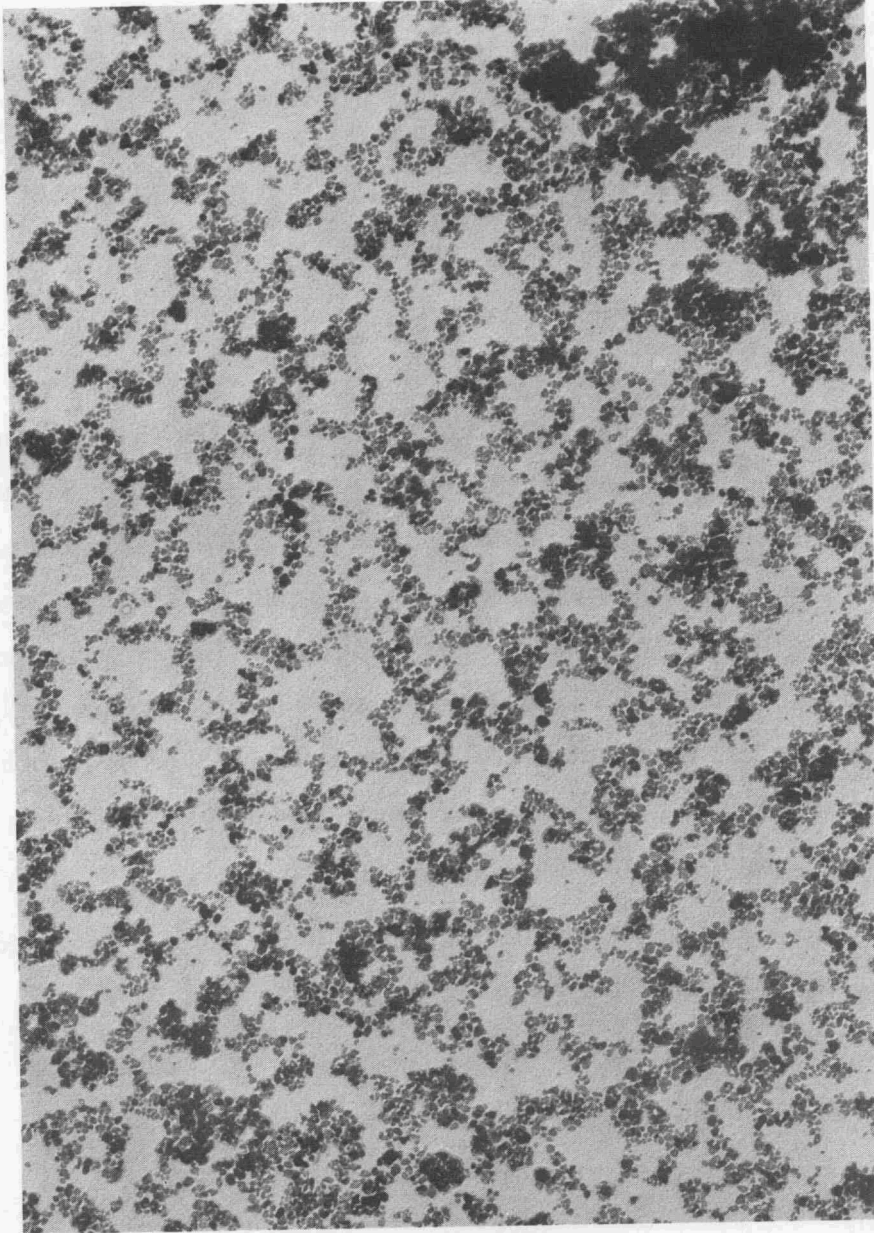
The aqueous thoria sol used in this program had been previously prepared in the Chemical Technology Division Pilot Plant by the standard ORNL procedure. In this procedure, thorium nitrate is steam-denitrated to give a hydrated oxide, which is then dispersed in dilute nitric acid by agitation and digestion.¹⁰ The x-ray crystallite size in these sols is typically 70 Å.¹¹ For the sol used in the work reported here, the BET surface area of the air-dried gel, 83 m²/g, gives a calculated crystallite size of 72 Å. An electron micrograph of this sol is shown in Fig. 1. From the photograph, the size of the individual particles is determined to be about 60 Å, which is in reasonable agreement with other measurements of size.

The sol used in this work is identified as Pilot Plant No. GS-44 and laboratory No. II-29. Analyses and properties are as follows:

ThO ₂ content	585.4 g/liter	(2.52 <u>M</u>)
NO ₃ ⁻ content	14.8 g/liter	(0.238 <u>M</u>)
NO ₃ ⁻ /Th mole ratio	0.095	
pH	3.4	
Viscosity	6 centipoises	

A pH dilution test indicated that the sol was slightly acid-deficient by about 0.01 in the acid/ThO₂ ratio. The sol was diluted to 2.0 M ThO₂ before it was blended with carbon.

ORNL PHOTO 92776



2000 A

Fig. 1. Electron Micrograph of ThO_2 Sol (Pilot Plant Sol No. GS-44).

2.1.2 Carbon

A proprietary pelletized channel black, Spheron 9* was used for virtually all the carbon black mixtures. The properties of Spheron 9 are listed below:

Fixed carbon (portion not volatilized at 1000°C in argon)	92.4%
BET surface area	105 m ² /g
Calculated particle size (from surface area)	300 A
pH of aqueous suspension	4.5

An electron micrograph (Fig. 2) of this carbon black shows rounded particles about 250 to 450 A in diameter; this size is in agreement with that calculated from the surface area.

In a few instances, other carbon blacks were used. These are characterized, as necessary, where they are mentioned.

An extra fine grade of graphite, a modified Great Lakes grade 1008, was supplied by J. M. Napier of the Y-12 Plant. It originally had a size of less than 150 μ, but had been reground and air-classified to less than 2 μ. The BET surface area, 16 m²/g, was equivalent to a calculated particle size of 0.2 μ. This material was 98.4% fixed carbon.

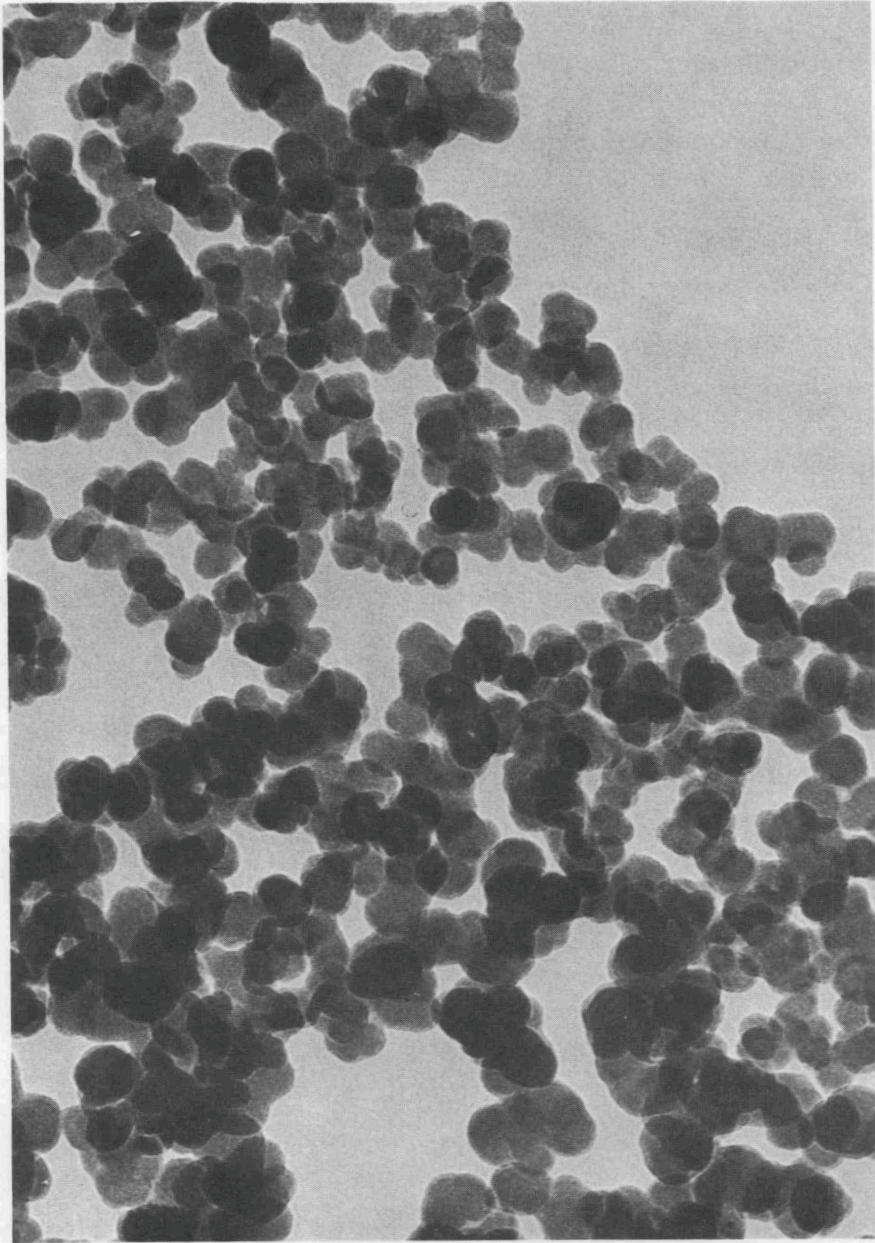
2.2 Preparation of Sols and Gels

2.2.1 Preparation of Sols

Mixed sols were produced in 100-ml batches by the ultrasonic blending of 2 M ThO₂ and the desired amount of carbon. Carbon contents, expressed as the C/ThO₂ mole ratio, varied between 0.1 and 6. These limits were selected on the basis that they should bracket the entire useful range, since a ratio of 0.1 was expected to yield a product with less than 3% porosity, while at a ratio of greater than 6 the viscosity

*Product of Cabot Corporation, Boston, Mass.

ORNL PHOTO 92777



2000 A

Fig. 2. Electron Micrograph of Spheron 9 Channel Black.

of the mixed sols becomes too high to allow the preparation of microspheres. The stated values of C/ThO₂ ratios are based on the fixed carbon content.

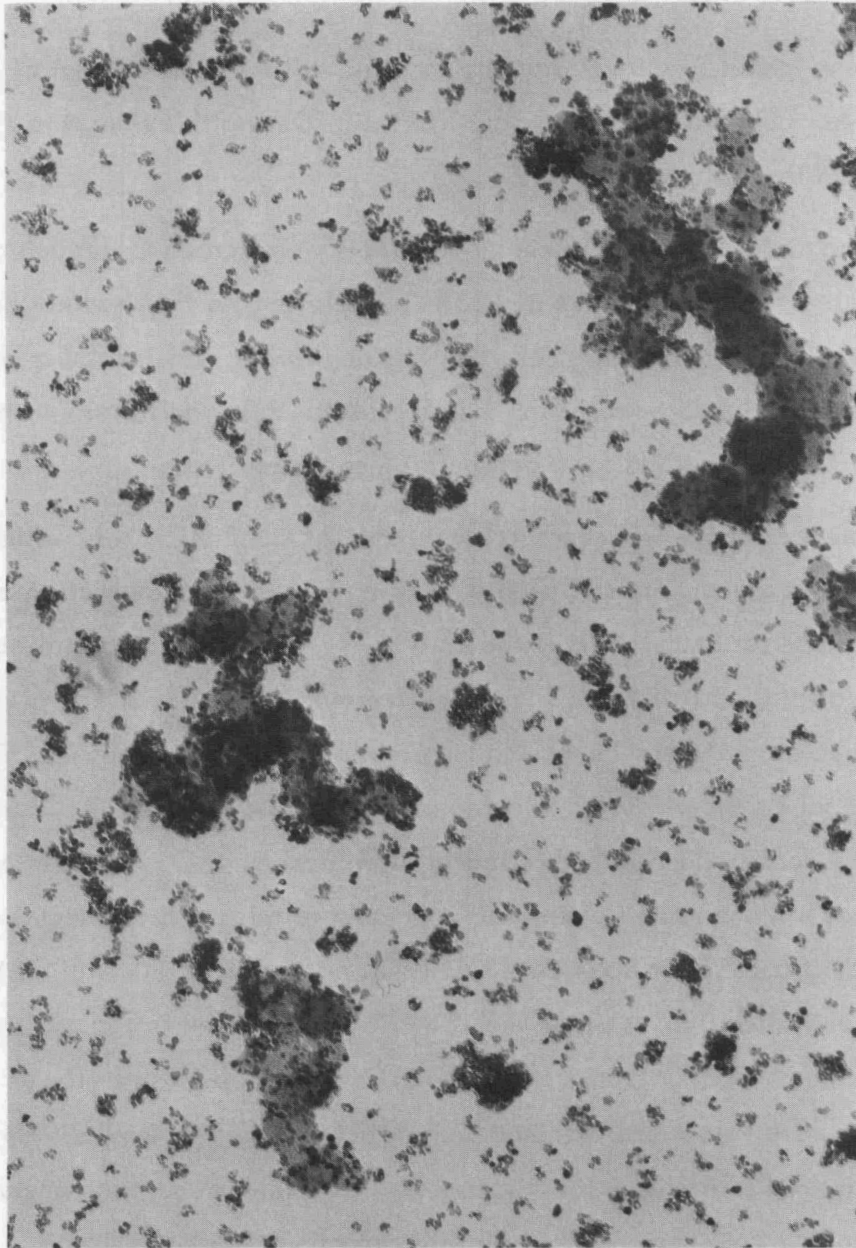
A Branson model S-110 ultrasonic generator, with a power output of about 110 watts at 20 kc, achieved good blending in 7 min. During this time, the dissipated energy heated the sol to about 60°C.

After the mixing step, the carbon-thoria sols were screened through a 100-mesh (149- μ openings) sieve to remove any carbon agglomerates that had not been incorporated in the sol. The quantity removed was negligible. Each sol was then poured into a bottle and placed on a rolling mill for 24 hr. After agitation on the mill, the sample was allowed to stand for a day before conversion to gel.

True sols are formed with carbon black and ThO₂. Similar sols, which have been on hand for over a year, are still stable. During the blending operation a carbon-thoria interaction disperses and stabilizes the carbon.¹² The thoria apparently acts as a protective colloid, partially coating the carbon particles (Fig. 3) and giving the mixed sol a positive zeta potential, even though carbon is normally negative. The effect of added ThO₂ sol on the viscosity of an aqueous suspension of carbon black is shown in Fig. 4. The viscosity decreases drastically when enough ThO₂ has been added to a thick paste of 8 M Spheron to "protect" the carbon; this decrease occurs at a C/ThO₂ mole ratio of about 7.5 for Spheron 9 and ThO₂ composed of 70-A crystallites. A reverse viscosity titration, starting with 2 M ThO₂, is shown in Fig. 5. Again, the "end point" occurs at a C/ThO₂ ratio of about 7. (The value is slightly lower in this case since the absolute values are twice as high as before; therefore relatively less "free" carbon is required to increase the viscosity.) The maximum carbon concentration used in the present work corresponds to a viscosity of about 70 centipoises.

Graphite did not form a sol with ThO₂, even though a decrease in viscosity similar to that described above was observed. Low-viscosity fluid suspensions were obtained, but, on standing overnight, some graphite settled out. Reagitation gave a suspension that was usable for gel formation. In the present work, only shards were prepared from graphite-thoria suspensions. It is possible to use such suspensions to form microspheres

ORNL PHOTO 92778



2000 A

Fig. 3. Electron Micrograph of ThO_2 -Spheron 9 Sol.

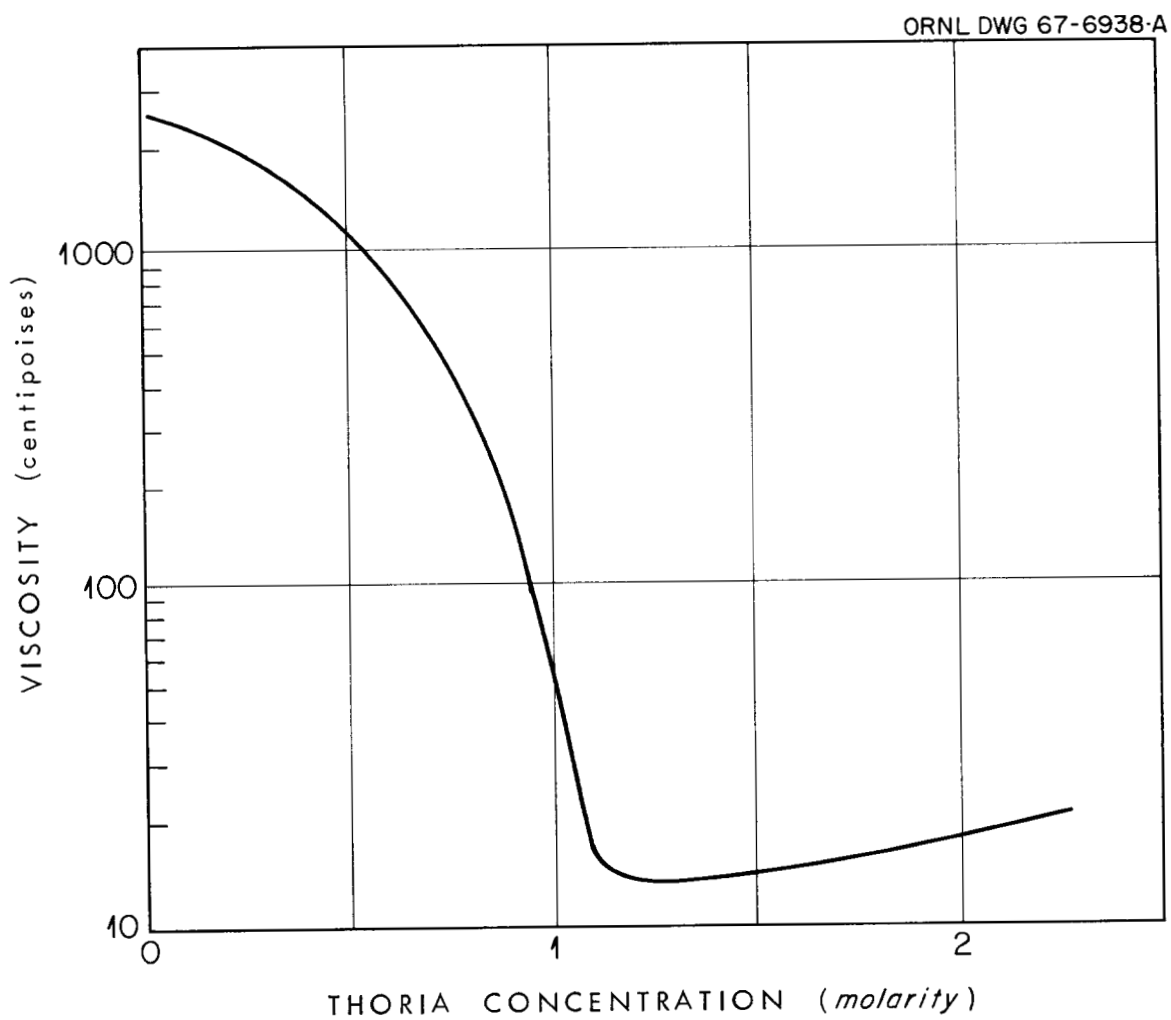


Fig. 4. Viscosity Titration of 8 M Spheron 9 with ThO₂ Sol.

ORNL DWG. 68-9619

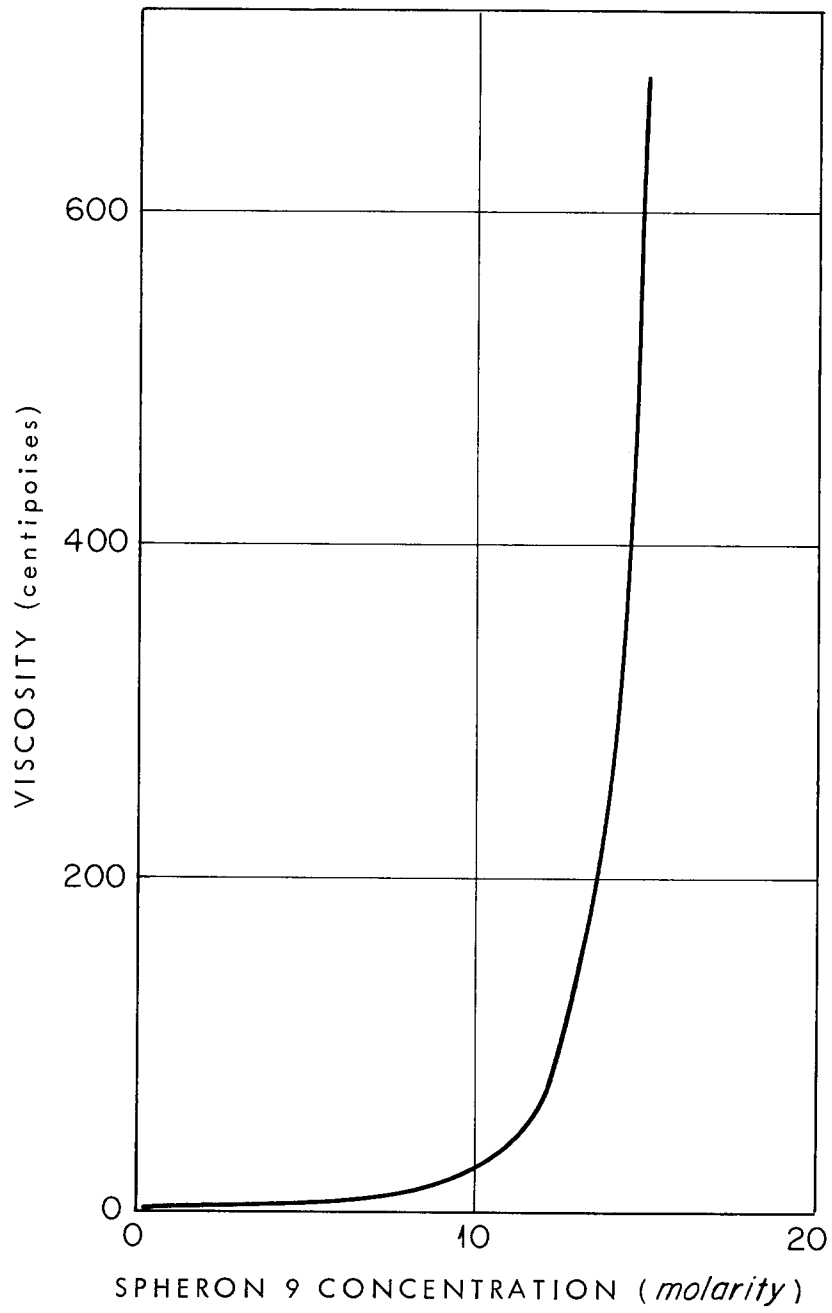


Fig. 5. Viscosity Titration of 2 M ThO_2 with Spheron 9.

in a column containing 2-ethyl-1-hexanol; however, previous work yielded microspheres of poor quality.

2.2.2 Preparation of Gels

Shards were prepared by pouring mixed sol (about 20 ml) into a petri dish and then drying it overnight at 110°C. The resulting fragments were crushed and screened, and the 10- to 80-mesh portion was retained for firing and porosity measurements.

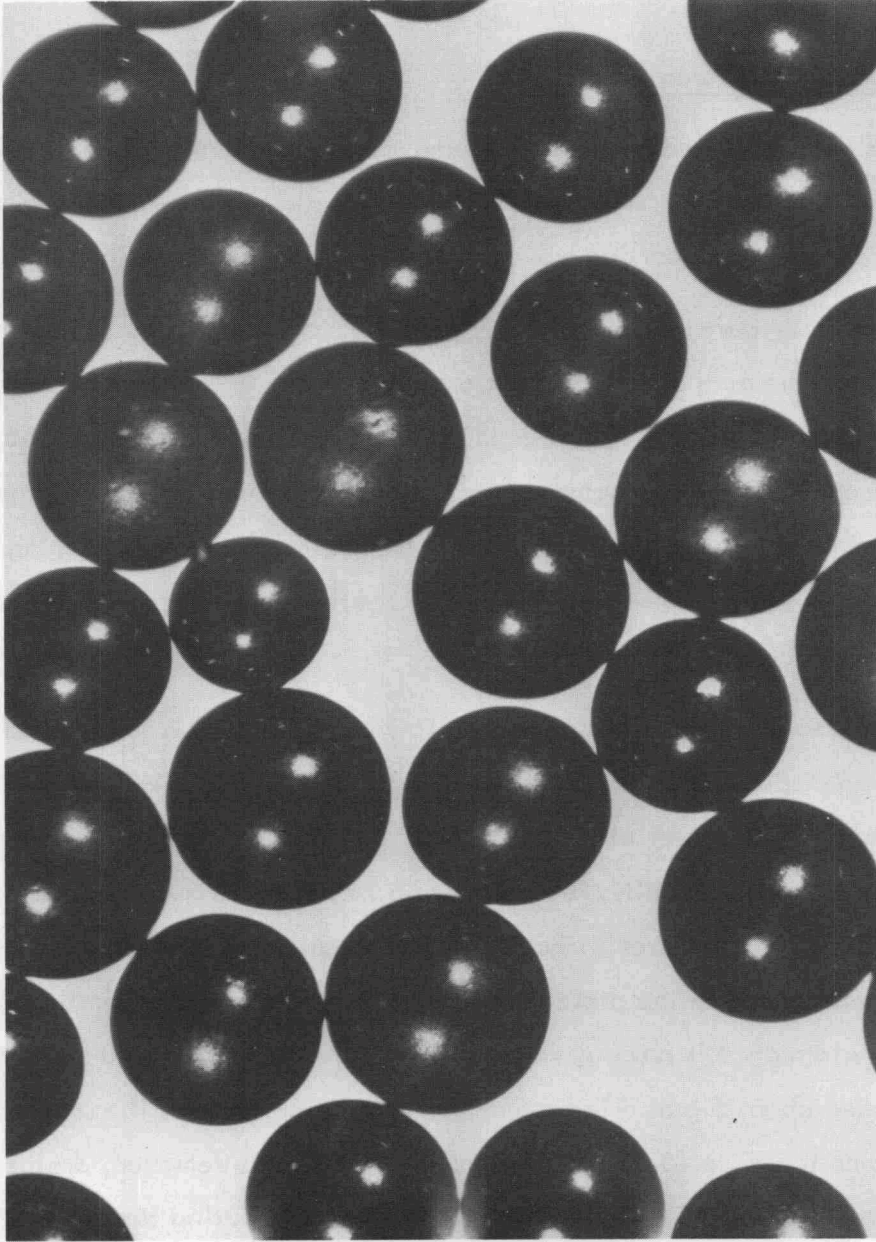
Microspheres were prepared in a 2-in. laboratory column by a previously described method.^{10,13} The dehydrating solvent used was 2-ethyl-1-hexanol. Two surfactants were required in order to obtain a good product: 0.2 volume % each of Span 80* and Ethomeen S-15.** The former controlled coalescence, while the latter was necessary to obtain smooth surfaces. Typical product microspheres are shown in Fig. 6. Microspheres could also be formed in a mixture of 2-ethyl-1-hexanol and 10% 2-octanol, plus 0.2% Span 80.

Standard sols formed microspheres quite well, with only a small amount of carbon being dispersed, or "shedded," to the organic phase. With unaged sols, that is, sols used immediately after ultrasonic blending, needle-plugging and excessive carbon shedding occurred. (Recently, in conjunction with other work, aged carbon-ThO₂ sols were formed into spheres without any carbon shedding. The solvent was nominally the same as that used in the present work. At this time, the explanation for the later, improved performance is not known.) Spheres were formed from 10-ml batches of sol, which yielded about 5 g of dried spheres. After being formed, the spheres were held in the column for 30 to 45 min to harden; then they were removed, drained, and oven-dried overnight at 110°C. Other work has shown that, during the sphere-forming step, adsorption of solvent causes an increase in the final C/ThO₂ mole ratio of about 0.2.¹⁴

*Sorbitan monooleate, marketed by Atlas Chemical Industries, Wilmington, Del.

**A tertiary amine, marketed by Armour and Company, Chicago, Ill.

Y-76619



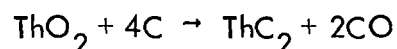
SIZE : APPROXIMATELY 90 X

Fig. 6. Typical C-ThO₂ Gel Microspheres.

2.2.3 Firing and Carbon Burnout

Because the surface area of unsintered thoria gel is quite high, this type of material tends to react with moisture and CO₂.¹⁵ Therefore, it was felt necessary to sinter the porous thoria produced in this program, at a temperature above 1000°C,¹⁶ at some time during the firing and burnout process. Carbon burnout at 800°C in air was selected on the basis that this temperature should be high enough to effect complete burnout in 1 hr or less, yet would be well below the sintering temperature. Two general methods were employed to accomplish sintering and burnout: (1) burnout at 800°C, followed by sintering at 1200, 1300, or 1400°C in air, and (2) sintering in an argon atmosphere at the latter temperatures, followed by burnout at 800°C. The rate of temperature rise used in the firing ovens was: 400°/hr to 800°, 300°/hr to 1100°, 200°/hr to 1300°, and 100°/hr to 1400°. Time at the final sintering temperature was usually 1 hr, but a few tests were made at shorter times.

The possibility of some conversion to carbide during the sintering of carbon-containing oxide was considered. The reaction



proceeds in vacuum above 1400°C. However, a very small overpressure of CO suppresses the reaction at this temperature. Under argon, a sufficient CO pressure is present from the reaction of oxygen complexed on the carbon surface to effectively prevent the formation of thorium carbide. None could be detected by qualitative testing (hydrolysis with dilute nitric acid).

After the program was under way, it was found that carbon burnout for some samples required much longer than 1 hr. These samples were low in added carbon and had been sintered before burnout. Where necessary, burning was continued for as long as 3 days; even this extended burning period did not always accomplish complete carbon removal.

2.3 Analytical Methods

The mercury intrusion technique¹⁷ was used to determine the porosity, the bulk density, and the high-pressure density of all samples. The measurements were performed with an Aminco porosimeter having a pressure limit of 15,000 psi (equivalent to a pore diameter of 120 A). The upper limit for diameters is 17 μ , at about 12 psi (absolute). From the sample weight and the initial volume, the bulk particulate density, that is, the density of individual particles including their internal void space, can be calculated. From the high-pressure volume, a final density can be obtained which excludes all void space penetrated by the mercury, that is, all open pores having diameters greater than 120 A. As an example of the excellent reproducibility of the method, results for two samples from the same lot, submitted three months apart, are shown in Table 1.

Table 1. Reproducibility of Measurements Made with Aminco Porosimeter

Sample No.	50-44 ^a	130a ^a
Porosity	4.21	4.43
Bulk density, g/cc	3.41	3.40
Final density, g/cc	3.56	3.56
Pore size distribution, % of total:		
120-190 A	39	41
190-350 A	28	31
350-870 A	13	17
870-2500 A	7	4
4-17 μ	13	7

^aTwo samples, submitted three months apart, from same lot of carbon-thoria shards. This material contains four moles of Spheron 9 per mole of thoria. The gel was dried at 110°C.

Helium densities, BET surface areas, porosities by nitrogen adsorption-desorption, and residual carbon contents were determined for selected samples. Helium displacement densities, when compared with the theoretical density, are useful for calculating the closed porosity; when compared with the high-pressure mercury density, they can be used to calculate the open porosity resulting from pores with diameters smaller than the lower limit (120 Å) by mercury intrusion. Nitrogen pore size distribution extends to a lower diameter limit of about 12 Å. Carbon was determined by combustion to CO₂ in a Leco apparatus at 1000°C.

Thermogravimetric analyses were performed on a conventional thermobalance at 1-atm pressure. A flow-through system provided the desired atmosphere. For programmed runs, a rise rate of about 5°C/min was used.

3. RESULTS AND DISCUSSION

Most of the work was done with shards in order to simplify the experimental program. The effects of the various parameters are, in general, clearly demonstrated with shards and can be extended to microspheres. However, some differences do exist, as described in Sect. 3.7. More work was done with carbon black than with graphite since the former yields a stable sol with thoria while the latter merely forms a suspension. Graphite, along with some carbon blacks other than Spheron 9, is discussed in Sect. 3.6. In the following sections, unless stated otherwise, the results are for shards prepared with Spheron 9.

3.1 Major Variables: C/ThO₂ Mole Ratio and Carbon Burnout Procedure

The primary effects of these two variables are shown in Fig. 7. The corresponding data are given in Table 2. The two burnout methods used in this test are as follows:

- (1) Burn carbon out at 800°C, then sinter at 1400°C for 1 hr;
- (2) Sinter at 1400°C for 1 hr, then burn out the carbon at 800°C.

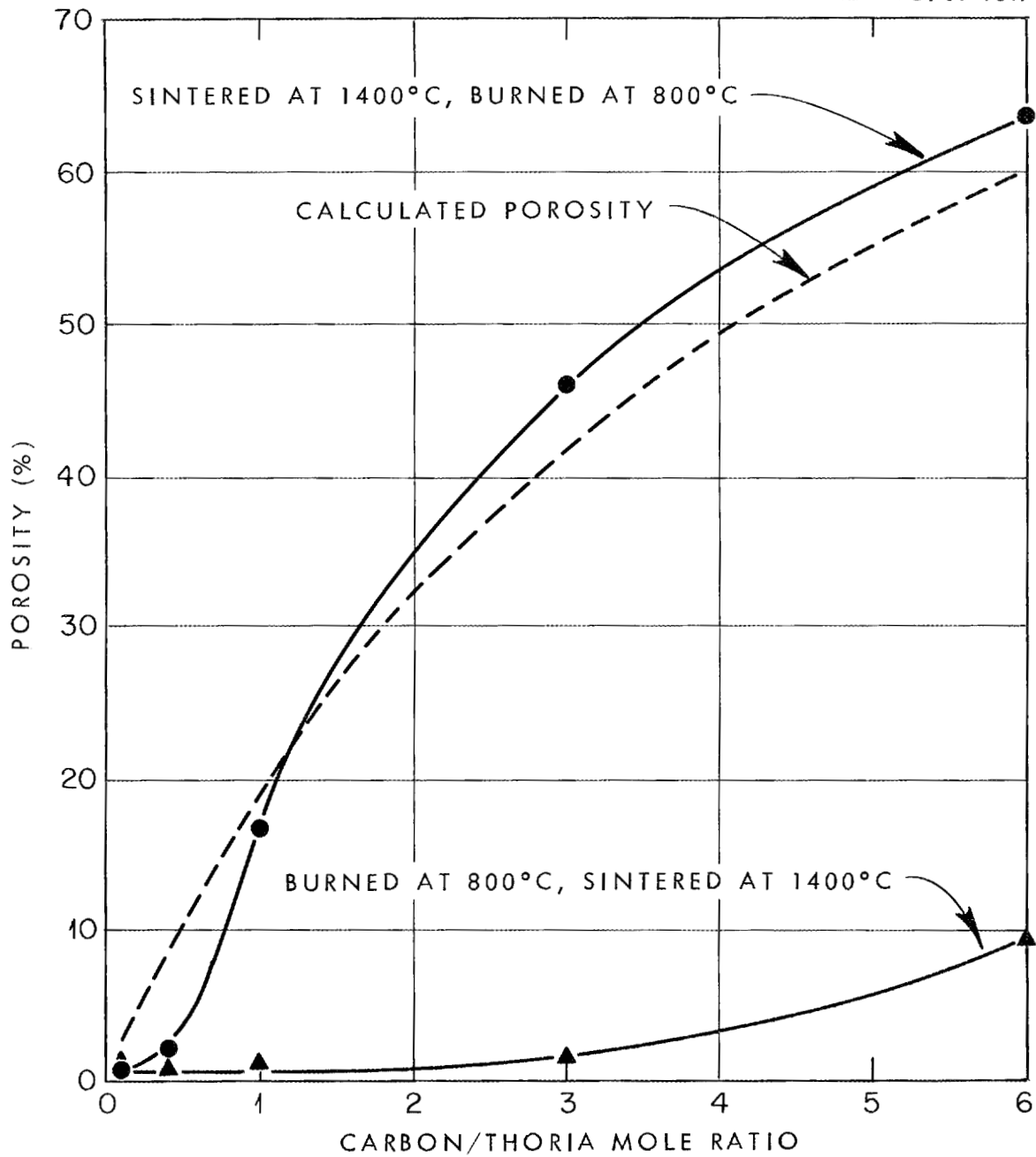


Fig. 7. Porosity as a Function of C/ThO₂ Mole Ratio and Carbon Burnout Procedure.

Table 2. Effects of C/ThO₂ Mole Ratio and Firing Schedule on Porosity and Density

Method	C/ThO ₂ Mole Ratio	Porosity (%)	Density ^a (g/cc)
1) Burnout at 800°C, followed by sintering at 1400°C	0.1	<1	9.88
	0.4	1	9.75
	1.0	<1	9.76
	3.0	2.0	9.42
	6.0	8.6	9.28
2) Sintering at 1400°C, followed by burnout at 800°C	0.1	<1	9.67
	0.4	2.8	9.35
	1.0	16.6	9.48
	3.0	46.7	9.50
	6.0	63.3	9.40

^aAt 15,000 psi. Therefore, only closed pores or pores smaller than 120 Å in diameter are included in this volume.

It is apparent from Fig. 7 and Table 2 that porosity is a direct function of the C/ThO₂ mole ratio. It is evident that high-temperature sintering followed by burning first "sets" the thoria matrix, after which the volume occupied by the carbon remains as open porosity, approximating the theoretical value. On the other hand, sintering after burnout is obviously quite effective in sintering out virtually all the porosity caused by carbon burnout, except at the highest C/ThO₂ mole ratio.

The calculated porosity curve (Fig. 7) is based on the assumptions that the thoria-carbon gel is nonporous before burnout and that the total volume occupied by the carbon is converted to measurable porosity. Thus,

$$\% \text{ porosity} = \frac{(100) \left(\frac{\text{amount of C present}}{\text{density of C}} \right)}{\left(\frac{\text{amount of C present}}{\text{density of C}} \right) + \left(\frac{\text{amount of ThO}_2 \text{ present}}{\text{density of ThO}_2} \right)}$$

By using 2.0 g/cc and 10.0 g/cc as the densities of carbon black and thoria, respectively, and converting to C/ThO₂ mole ratio (R), the above equation becomes:

$$\% \text{ porosity} = 6000R / (60R + 264) .$$

Since the experimental C/ThO₂ mole ratios were calculated on the basis that Spheron 9 is 92.4% fixed carbon, the above equation must be corrected by dividing both R terms by 0.924 in order to obtain the curve in Fig. 7.

For the sinter-burn method, the observed porosity approximates the calculated value; negative deviations occur at C/ThO₂ ratios below 1.0, and positive deviations occur above 1.0. When the simplified assumptions made in calculating the curve are considered, the deviations are surprisingly small. The positive deviations are readily explained by recognizing that the unfired gel must have contained some porosity, and that part of this was retained by the final product. The negative deviations at a low C/ThO₂ mole ratio are not so easily explained, particularly since the mercury densities are nearly theoretical (see below). It is unlikely that the ThO₂ sintered after carbon burnout at 800°C. Perhaps some carbon was lost during sintering due to inleakage of air.

The mercury densities at 15,000 psi, that is, the densities after all open pores with diameters greater than 120 A have been penetrated by mercury, are also listed in Table 2. None of the samples attained the theoretical density of 10.03 g/cc. The four samples whose open porosities were less than 2% have densities 97 to 99% of theoretical, while the remaining samples, with measurable porosities of 2% or more, have densities that are only 93 to 95% of theoretical. Thus, introduction of any significant amount of open porosity also introduces 5 to 7% closed, or <120 A porosity, which is not measurable by mercury intrusion.

Table 3 gives the pore size distribution for the three high-porosity samples of Table 2. None of the pores in each of these samples is greater than 1000 A in diameter. The size distribution for the samples are relatively narrow, with 89% of the pores in the 120- to 190-A range at 17% porosity, 88% in the 250- to 350-A range at 47% porosity, and 79% in the 250- to 580-A range at 63% porosity. Thus, as the porosity

Table 3. Pore Size Distribution for High-Porosity Samples Listed in Table 2

	C/ThO ₂ Mole Ratio		
	1.0	3.0	6.0
Total porosity, %	17	47	63
Total porosity in size range indicated, %			
0.1 - 17 μ	0	0	0
580 - 1000 A	5	0	13
350 - 580 A	2	1	37
250 - 350 A	2	88	42
190 - 250 A	2	9	6
120 - 190 A	89	2	2

increases, the average pore size also increases and the range seems to become broader.

For the low-porosity (2.0 to 8.6%) samples in Table 2, the distribution trend of Table 3 is reversed; that is, the pore sizes are larger, with about 90% of the total pore volume greater than 1000 A and 43 to 65% in the 3- to 17- μ range.

3.2 Minor Variables and Reproducibility

By definition, minor variables are those which have relatively little or no effect on the porosity of the ThO₂ product. As will be shown, these variables include: the method of sol preparation, the method of gel preparation, and the size fraction of the shards. During the early part of the test program some extreme cases of nonreproducibility were noticed; therefore, a rather extensive series of tests was conducted to determine the degree of reproducibility that could be expected routinely. In addition to the deliberate variables mentioned above, the effects of a change in operator and of sample preparation in duplicate by the same operator were also checked and found to be of minor importance. The data obtained are summarized in Tables 4 and 5 for

Table 4. Effects of Minor Variables on Reproducibility of Preparation Having a C/ThO₂ Mole Ratio of 1.0

Sample No.	Porosity (%)	Density ^a (g/cc)
3-1	2.9	9.09
3-9	18.1	9.48
3-10	17.4	9.50
3-11	16.4	9.48
3-12	16.6	9.46
3-2-R	20.2	9.53
3	16.6	9.38
III-44-A-1	19.5	9.62
B-1	19.4	9.52
C-1	18.3	9.53
D-1	19.3	9.51
III-45-A-1	16.8	9.42
B-1	17.4	9.47
C-1	17.2	9.49
D-1	18.0	9.46
III-55-C-1	18.3	9.52
D-1	18.4	9.55

^aMercury porosimeter measurements at 15,000 psi.

Table 5. Effects of Minor Variables on Reproducibility of Preparations Having a C/ThO₂ Mole Ratio of 3.0

Sample No.	Porosity (%)	Density ^a (g/cc)
4-1	10.0	9.46
4-7	47.4	9.61
4-8-A (>10 mesh)	45.2	9.44
4-8-B (10-20 mesh)	45.5	9.46
4-8-C (20-80 mesh)	46.2	9.54
4	46.7	9.57
III-44-A-3	48.7	9.56
B-3	49.1	9.36
C-3	48.5	9.44
D-3	48.7	9.54
III-45-A-3	47.5	9.55
B-3	47.4	9.51
C-3	47.7	9.56
D-3	47.0	9.53
III-55-C-3	46.6	9.45
D-3	46.5	9.54

^aMercury porosimeter measurements at 15,000 psi.

C/ThO₂ mole ratios of 1.0 and 3.0, respectively. In all cases the firing procedure used was sinter-burn, as described earlier.

The nonreproducibility mentioned above is shown by samples 3-1 and 4-1. One other sample (No. 5-1, not included in the tables) also showed extreme deviation. At a C/ThO₂ mole ratio of 6.0, it had a porosity of only 23% vs a norm of 64%. At the time this problem appeared there was no obvious explanation. It is now believed that aberrations in the firing cycle were probably responsible for the very low porosities observed for these three samples. During the first few preparations, the method of changing from sintering to burning temperature was not standardized, and these three samples were probably burned at temperatures well above 800°C. Samples 3-1 and 4-1 will not be included in the following discussion.

Three different persons prepared the samples listed in Tables 4 and 5. Numbers 3-1 through 3-12 (Table 3) and 4-1 through 4-8-C (Table 5) were prepared by C. K. Neulander, while 3-2-R, 3, and 4 were prepared by A. H. Mesch. The remainder were prepared by the author. No significant trend is observed as a result of the change in operators.

Samples 4-8-A, 4-8-B, and 4-8-C represent three different sieve size fractions of the same gel. The total variation in porosity, 1%, for these samples is only one-fourth of the total deviation shown by all the samples in Table 5 and is not significant. It is interesting to note that within this series both the porosity and the mercury density increase slightly as the particle size decreases. These increases occur because a greater portion of the porosity that is inaccessible to mercury is exposed as more surface is made available. However, the smallness of this trend shows that the bulk of the porosity, which is open, is readily accessible.

Likewise, variations in the mechanics of sol preparation and gel formation are shown to have an insignificant effect on porosity. The III-44 and III-45 series represent four methods of sol handling. The overall scheme is as follows:

- A. Blend Spheron 9 and ThO₂ sol by ultrasonic agitation for 7 min.
- B. Tumble for 24 hr.

C. Let stand for 24 hr.

D. Blend again by ultrasonic agitation for 7 min.

Samples designated A, B, C, and D (Tables 4 and 5) were gelled immediately after each of the corresponding operations. Within a given series, the maximum variation in porosity was 1.2%, which is not significant when compared with the total variation at either C/ThO₂ mole ratio.

The III-55 samples involve two different gelation procedures. The standard method is drying overnight at 110°C. The "C" samples were allowed to gel very slowly by evaporation at about 50°C, while the "D" samples were gelled very rapidly (about 3 min) by heating on a hot plate. Again, no differences in porosity were found.

The only significant variable causing a change in porosity was the preparation of a new batch of sol, that is, weighing out carbon, measuring a volume of ThO₂ sol, and combining the two materials. Table 4 shows that the average porosity of the III-44 series samples, all of which were prepared from the same blended sol, is $19.1 \pm 0.4\%$; for the III-45 samples, the average is $17.4 \pm 0.4\%$; and for the III-55 samples, it is $18.35 \pm 0.05\%$. The corresponding figures from Table 5 are $48.7 \pm 0.2\%$, $47.4 \pm 0.2\%$, and $46.55 \pm 0.05\%$. The variation from series to series is significantly greater than the variation within a series. Similarly, the variations from series to series in the 3- and 4- samples are greater than the variation within a series. The following groups (shown in parentheses) were prepared from different sols: (3-9, -10, -11, -12), (3-2-R), (3), (4-7), (4-8-A, -B, -C), (4). The 3-9, -10, -11, and -12 samples involve differences in gelation procedure. The magnitude of these differences is less than that for the III-44 and III-45 series.

In preparing duplicate sols, small errors in weighing or in volume measurements cause variations in the C/ThO₂ mole ratio. Assuming conservatively that the weighings, which were made on a triple beam balance, are accurate to ± 0.1 g and that the volumes measured in a 100-ml graduate are accurate to ± 2 ml, the resultant variations in the C/ThO₂ mole ratio are ± 0.06 at a value of 1.00, and ± 0.10 at 3.00. From the slope of the curve in Fig. 7, $(\Delta \text{porosity}) = 27 (\Delta \text{ratio})$ at $R = 1$ and $(\Delta \text{porosity}) = 9 \cdot$

(Δ ratio) at $R = 3$, from which the porosity limits are calculated to be $\pm 1.6\%$ at $R = 1$ and $\pm 0.9\%$ at $R = 3$. These values are in reasonable agreement with the actual ranges of $\pm 1.9\%$ observed at C/ThO₂ mole ratios of both 1 and 3. The extra range observed experimentally includes other sources of error in addition to initial measuring errors. For example, a varying amount of carbon is always lost on the walls of the mixing vessel and on the ultrasonic probe. Direct analysis for carbon and thoria gives a ratio that is accurate to only ± 0.1 and is, therefore, useless for direct verification of the preceding explanation of the observed variations. Assuming the validity of the above argument, it should be possible to control the porosity more closely by working with larger batches and using more precise measuring and weighing techniques.

Ultrasonic blending was used to prepare all the mixed sols in the present work. However, one of the trial porosity samples mentioned earlier⁸ was made from a sol which had been blended on a ball mill. This material had a C/ThO₂ mole ratio of 2.1 and a mercury porosity of 37%. This compares favorably with the data given in Fig. 7, which shows a porosity of 35% at a C/ThO₂ ratio of 2.1.

All the mercury densities listed in Tables 4 and 5 are in the range of 93 to 96% of theoretical, thus indicating 4 to 7% of either closed and/or very fine porosity. The same observation was made earlier, based on the data in Table 2. There is no observable trend in Tables 4 and 5 to suggest that density per se is related to any of the minor variables discussed in this section.

3.3 Other Factors Related to Firing Schedule

3.3.1 Variations in Firing Cycle

The major effect of the firing cycle in terms of burn-sinter vs sinter-burn (sintering at 1400°C and burnout at 800°C) has already been discussed in Sect. 3.1. The use of lower sintering temperatures and the effect of time are other factors that should be considered briefly.

Table 6 lists the porosities and pore size distributions resulting from sintering temperatures of 1200, 1300, and 1400°C. Measurements were obtained at C/ThO₂ mole ratios of 0.4 and 3. Both types of firing cycles were used: (1) burn-sinter and (2) sinter-burn.

With firing cycle (1), at a C/ThO₂ mole ratio of 3, a lower sintering temperature has two effects: it results in a greater porosity, and it shifts the pore size distribution toward smaller sizes. However, even at 1200°C, the total porosity is only about 23% that obtained with cycle (2). At a C/ThO₂ ratio of 0.4, no effect was noted over the 1200-1400°C temperature range with firing cycle (1).

With cycle (2), the product properties are not affected by temperature, except for a shift to smaller pore sizes at the lower sintering temperatures. Sample No. 4-4 (see Table 6) is obviously in error.

Table 7 shows that decreasing the sintering time from 1 to 0.5 hr at 1400°C has no appreciable effect on the porosity. In later work with spheres, one sample was inadvertently given "zero" exposure time, as compared with a standard 1-hr exposure, at 1400°C without affecting the porosity. It must be remembered that with the heating program used, all samples are exposed to lower temperatures for significant times (see Sect. 2.2.3).

Three samples were prepared by sintering and burning in a single step, at 1400°C in air. As would be expected, the resulting porosities were intermediate between the values obtained by using firing cycles (1) and (2). Obviously, the heating rate and the availability of oxygen are governing factors in the combined method. Difficulty in controlling the porosity would be expected for this method.

3.3.2 Thermal Stability of Product

The thermal stability of porous thoria made by using firing schedule (2) (i.e., sintered at 1400°C and burned at 800°C) was determined by subsequent exposure to temperatures of 1000, 1100, 1200, 1300, and 1400°C for 1 hr. The results for two

Table 6. Effect of Sintering Temperature

Sample No.	Carbon to-Thoria Ratio	Temperature	Porosity (%)	Pore Size Distribution (%)				
				17.2-3 μ	3-0.5 μ	0.5-0.1 μ	1000-250 A	250-120 A
<u>(1) Burning in Air at 800°C, Followed by Sintering in Air at Temperature Indicated</u>								
2-2	0.4	1400	1	-	-	-	-	-
2-3	0.4	1300	<1	-	-	-	-	-
2-5	0.4	1200	<1	-	-	-	-	-
4-2	3	1400	1.98	60	24	8	8	0
4-3	3	1300	2.78	43	33	17	8	0
4-5	3	1200	10.92	22	28	20	3	27
<u>(2) Sintering in Argon at Temperature Indicated, Followed by Burning in Air at 800°C</u>								
2-1	0.4	1400	2.82	65	21	0	7	7
2-4	0.4	1300	1.78	67	8	8	0	17
2-6	0.4	1200	1.49	60	20	0	20	0
4	3	1400	46.68	0	0	0	89	11
4-4	3	1300	(33.84)	2	0	0	0	98
4-6	3	1200	46.73	1	0	0	3	97

Table 7. Effect of the Length of Time at Sintering Temperature

The carbon was burned out according to the Schedule: Sintering at 1400°C for the time specified, followed by burnout at 800°C.

Sample No.	Carbon To-Thoria Ratio	Time (hr)	Porosity (%)	Pore Size Distribution (%)			
				17.2-3 μ	3-0.5 μ	0.5-0.1 μ	1000-120 A
2-1	0.4	1	2.82	65	21	0	14
2-7	0.4	0.5	3.17	34	3	3	60
4	3	1	46.68	0	0	0	100
4-7	3	0.5	47.36	0	2	0	98

levels of porosity are given in Table 8. Above 1100°C, sintering begins; at 1200°C, about 20 to 30% of the original porosity has been lost; at 1300°C, virtually all the porosity has been sintered out.

Table 8. Effect of Post-Sintering on Porous Thoria

	C/ThO ₂ Mole Ratio	
	1.0	3.0
Porosity, %		
Initially	19	48
After Firing at:		
1000°C	19 ^a	47
1100°C	18 ^a	45
1200°C	15	32
1300°C	<1	1.5
1400°C	<1	<1

^aThese values include corrections to compensate for measurements made to only 10,000 psi (rather than the usual 15,000 psi) because of equipment difficulties.

3.4 General Structure

A better understanding of the general structure of porous thoria can be obtained from other physical measurements such as helium density, nitrogen adsorption/desorption, hardness, and surface area.

3.4.1 Density, Pore Size Distribution, and Hardness

It has already been seen that, for samples with 2% or more open porosity, the mercury density at 15,000 psi is only 93 to 95% of theoretical (Sect. 3.1). Helium densities on four such samples are as follows:

<u>Sample No.</u>	<u>Helium Density (g/cc)</u>
44-C-1	9.94
45-C-1	9.80
44-C-3	10.10
45-C-3	9.94

Since the helium densities are 98 to 100% of theoretical, the "missing" 5 to 7% not found by mercury intrusion is actually present as open pores that are smaller than 120 A in diameter. For samples of less than 2% measured porosity, the final mercury density is 97 to 99% of theoretical. The mercury density of one sample of nonporous ThO₂, prepared during this program (i.e., no carbon was added), was 9.91 g/cc, or 99% of theoretical.

The pore size distribution of several samples was obtained by N₂ adsorption/desorption. (This service was provided by Paul Dake, ORGDP.) These measurements were obtained for two reasons: to check on the pore-size distributions as determined by the mercury method, since the two methods overlap; and to determine the size distribution of the 5 to 7% porosity referred to above (which is below the range of the mercury method) by the nitrogen method. Figures 8 and 9 compare, graphically, the results obtained by both methods for samples 45-B-1 and 45-B-3. In general, agreement between the two methods is excellent.

For sample 45-B-1, the Hg porosity is 17.5%, and the final density implies an additional 5.5% porosity, for a total of 23%. The N₂ porosity of 21% thus indicates 2% closed porosity, while the Hg value, after correction for 2% porosity below a diameter of <120 A, gives 3.5% closed porosity. Correcting the N₂ value for the 2% porosity below 120 A gives 19% above 120 A, or 1.5% greater than the Hg value.

For sample 45-B-3, neither method shows any porosity below 120 A. The two direct values are 47.5 and 49%, with the N₂ value again being 1.5% high. Adjusting the Hg value to compensate for the final density gives 52% porosity, which indicates 3% closed porosity vs the N₂ value, or 4.5% vs the Hg porosity.

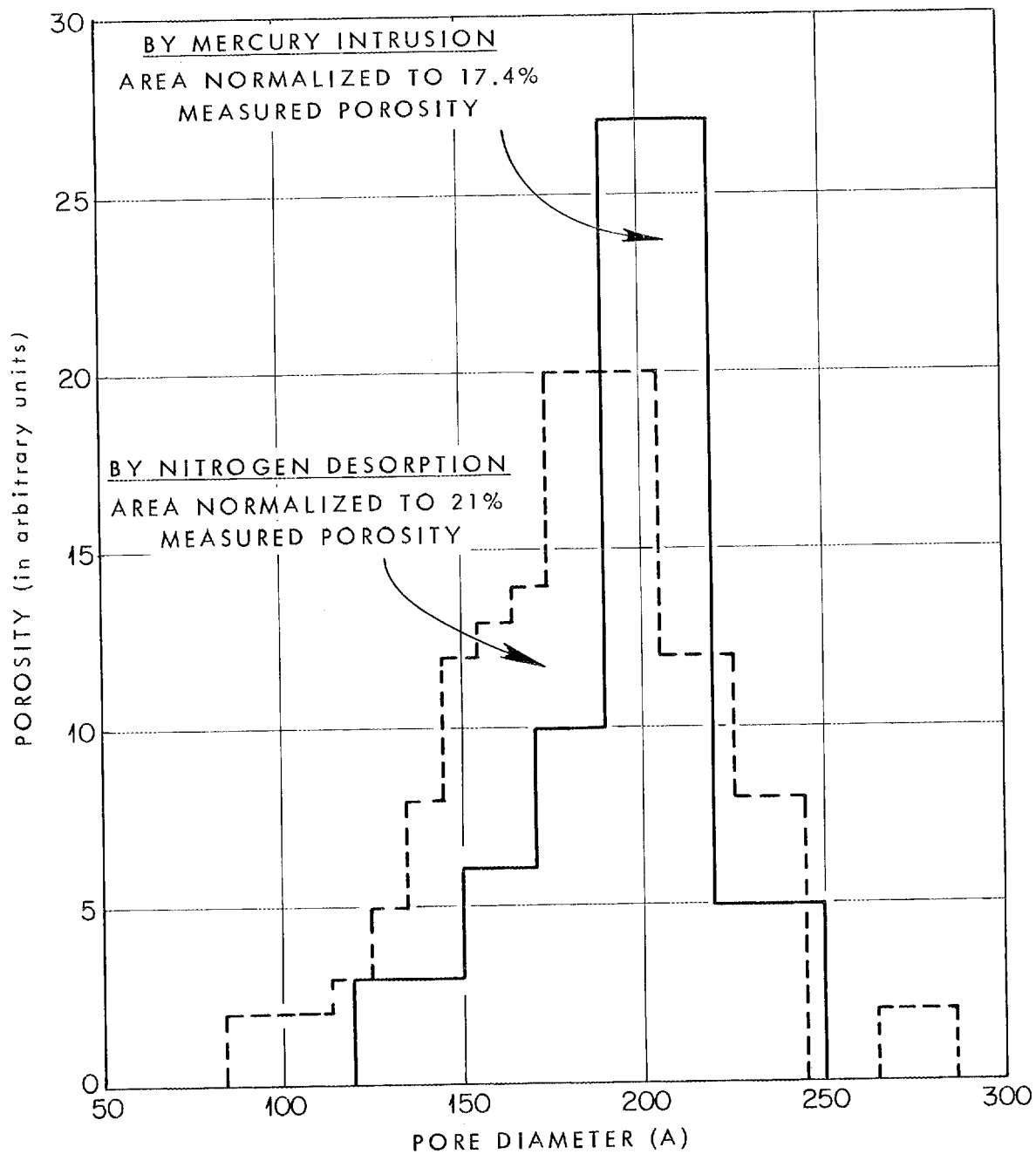


Fig. 8. Pore Size Distribution for Sample 45-B-1, as Determined by the Mercury and the Nitrogen Methods.

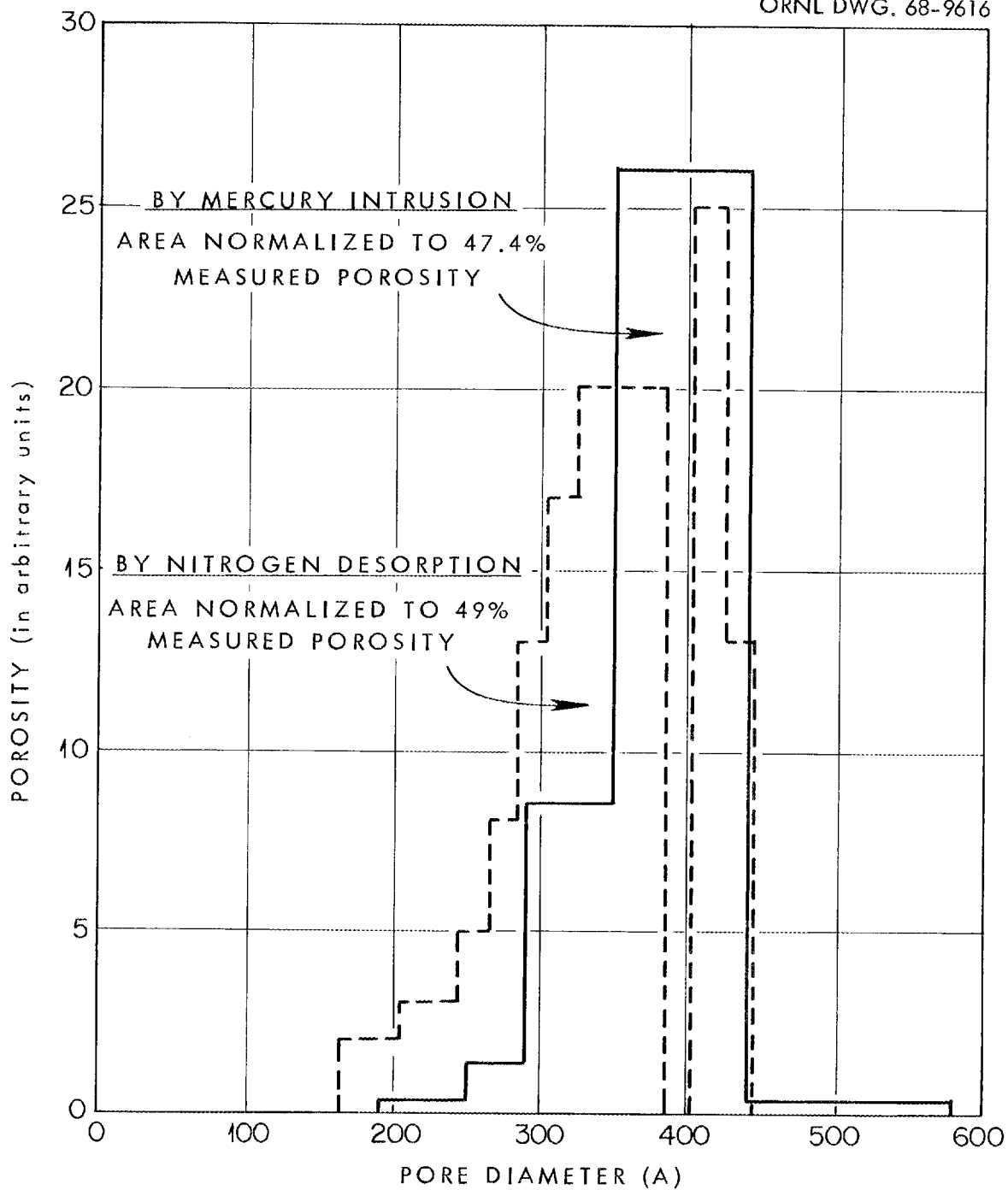


Fig. 9. Pore Size Distribution for Sample 45-B-3, as Determined by the Mercury and the Nitrogen Methods.

The pore size distribution of different samples is a function of both total porosity (i.e., original carbon content) and firing cycle. (This was discussed in Sect. 3.1 for samples sintered at 1400°C.) Similar results were obtained for the reproducibility series samples (Tables 4 and 5). At a C/ThO₂ mole ratio of 1.0, the diameters of the pores averaged 180 to 240 Å, with ranges of 120/220 Å to 150/290 Å, while at a C/ThO₂ ratio of 3.0, the pores centered at 300 to 400 Å with ranges of 250/440 Å to 300/460 Å. Thoria with large pores was obtained only at porosities of less than 11%. Using a sinter-burn schedule at a C/ThO₂ ratio of 0.4, 3% porosity was obtained in the micron range. With a burn-sinter schedule, pores in the micron range resulted. A greater degree of porosity was obtained at the highest carbon contents for a constant sintering temperature of 1400°C (up to 8.5%) or at lower sintering temperatures for constant carbon content (up to 11%).

Hardness measurements were made on two porous thoria samples, as follows:

<u>Sample No.</u>	<u>% Porosity</u>	<u>Diamond Point Hardness</u>
44-B-3	49	69
44-B-1	19	572

From the Knoop hardness for dense thoria,¹⁸ a D.P.H. of 630 is calculated. It is rather surprising that the 19% porous thoria is almost as hard as the dense material. At 49% porosity, the hardness decreased by almost 90%.

Figures 10 and 11 are photomicrographs (100X) of samples 44-B-3 and 44-B-1, mounted in epoxy resin. The resin has penetrated into the body of each fragment, to a depth of about 50 μ for the 19% porous sample and about 120 μ for the product with 49% porosity. In both cases, the oxides appear to be dense, because the pores are far too small to be observed microscopically.

3.4.2 Surface Area and Structure

Surface areas were obtained for: (1) air-dried carbon-thoria gels, (2) 1400°C-sintered material, and (3) sintered and burned oxide. The first two sets of measurements

Y-76664

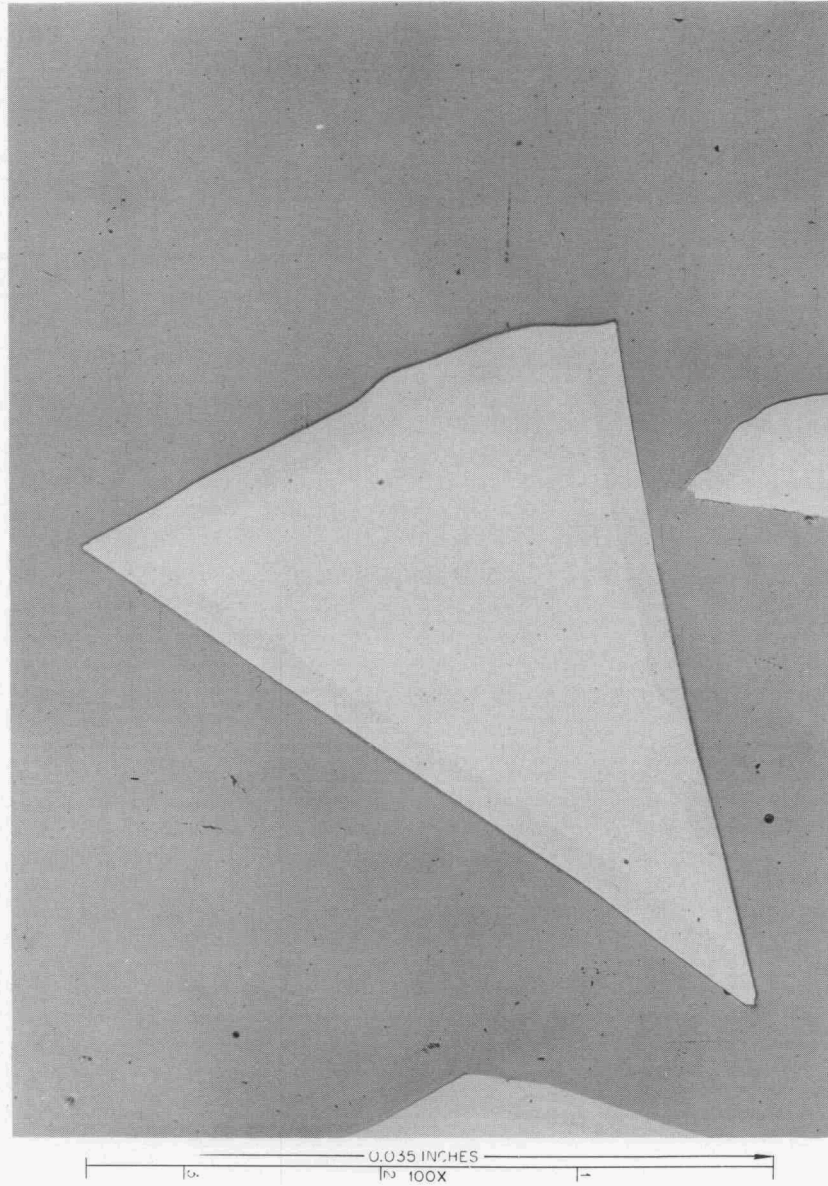


Fig. 10. Cross Section of Sample 44-B-1, Mounted in Epoxy Resin. 100X.

Y-76665

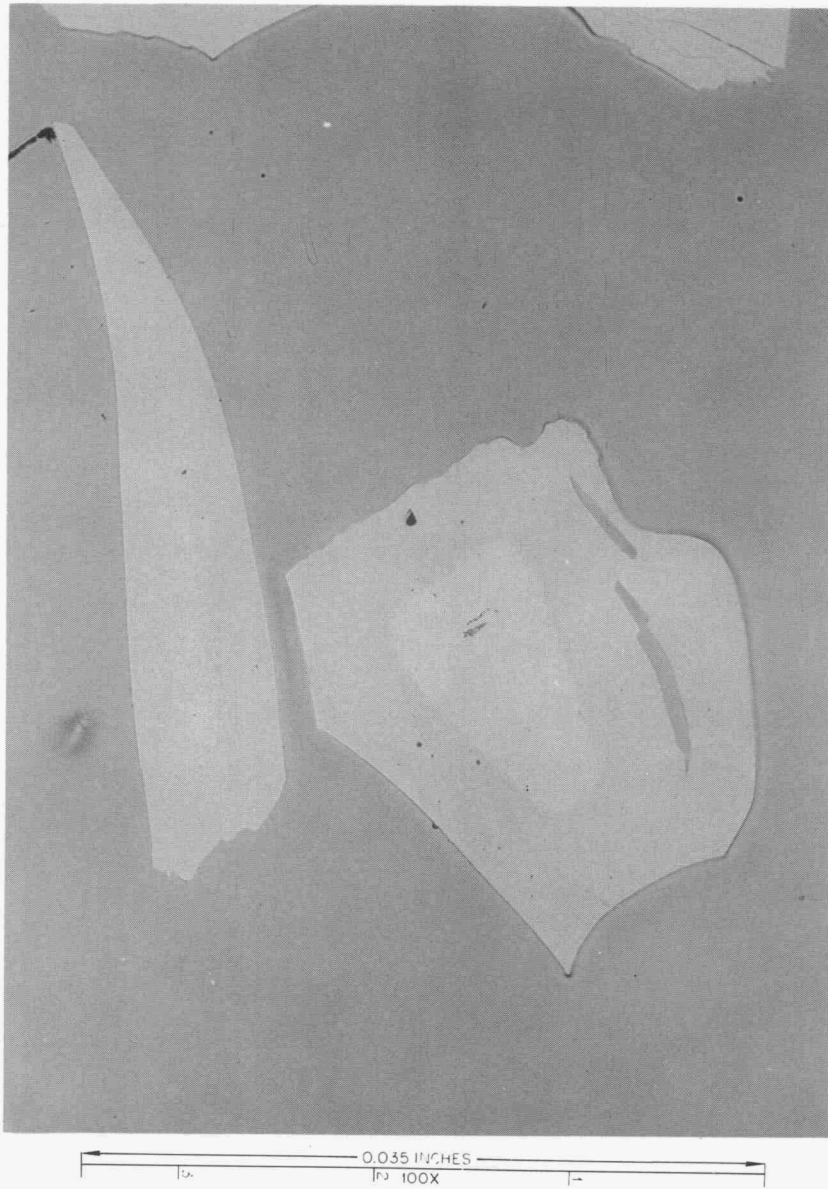


Fig. 11. Cross Section of Sample 44-B-3, Mounted in Epoxy Resin. 100X.

were obtained previously for gels having a C/ThO₂ mole ratio of 4, but the results are also applicable here. The third set of data was obtained from some of the samples prepared for the post-sintering study (Table 8); the samples used were those treated at temperatures of 1000°C and 1100°C.

Table 9 lists the experimental (BET) and calculated specific surface areas for five different air-dried gels, representing three different carbon blacks and three different blending methods. The calculated values are based on simple addition of the ThO₂ and carbon areas, using 15 wt % carbon and 85 wt % ThO₂ for the composition. The individual specific surface areas used for the calculations were:

ThO ₂	86 m ² /g (70-A crystallites)
Spheron 9	105
Sterling L	30
Neospectra Mark II	1000

The agreement between calculated and experimental values serves to verify the addition method used in the calculation. On this basis, it can be assumed that the "protective" action of thoria on carbon black to form stable sols neither creates nor destroys surface area, and that the resulting gels are porous enough to permit complete penetration by nitrogen. An idealized model of such a gel might be such as that shown in Fig. 12, where the large spheres are carbon, the cubes are thoria, the relative carbon size shown is for Spheron 9, and the relative amounts of carbon and ThO₂ represent a C/ThO₂ mole ratio of 7.5 (the titration end point in Fig. 5).

Sintering the air-dried carbon-thoria gels (Table 9) in argon at 1400°C caused their specific surface areas to decrease to 13, 17, 17, 10, and 81 m²/g respectively. These areas are still quite high in view of the thermal treatment. In an effort to establish a basis for calculating the areas of these sintered gels, several models were considered; however, none gave a systematic agreement with all the observed values. This failure is probably due to real differences in the actual sintering of the thoria in the presence of such widely differing carbon blacks as those listed in Table 9.

Table 9. Surface Areas of Five Air-Dried Carbon-Thoria Gels

C/ThO₂ mole ratio = 4

Carbon Black	Blending Method	Surface Area (m ² /g)	
		BET	Calculated
Spheron 9	Ball mill	90	89
Spheron 9	Ultrasonic	91	89
Spheron 9	Pump loop	87	89
Sterling L	Ball mill	77	76
Neo. Mark II	Ball mill	223	250

Figure 13 shows one possible model in which the thoria is assumed to sinter into a shell around each carbon particle. The resulting area would be the external area of the double spheres. On this basis, the calculated areas for the three types of carbons (see Table 9) would be 25, 7.6, and 54 m²/g, respectively. These values are higher, lower, and lower, respectively, than those actually observed. Another possible model involves the assumption of the loss of all ThO₂ area due to sintering, so that only the carbon area contributes to the total area of the fired gel. This method gives values of 16, 4.5, and 150 m²/g, which are approximately correct, low, and high, respectively, when compared with observed values. In actuality, some combination of the features of these two models, whereby the thoria forms an irregular matrix in and around the carbon, would provide greater accuracy.

Table 10 gives the surface areas and other porosity data for four samples of sintered and burned porous ThO₂. For a given C/ThO₂ mole ratio, the surface area is reproducible. The calculated areas are based on the assumptions that the total pore volume is present entirely as average-sized pores and that the total area of spherical pores is measurable. The latter assumption will obviously give a high result, since the

ORNL DWG 68-9434

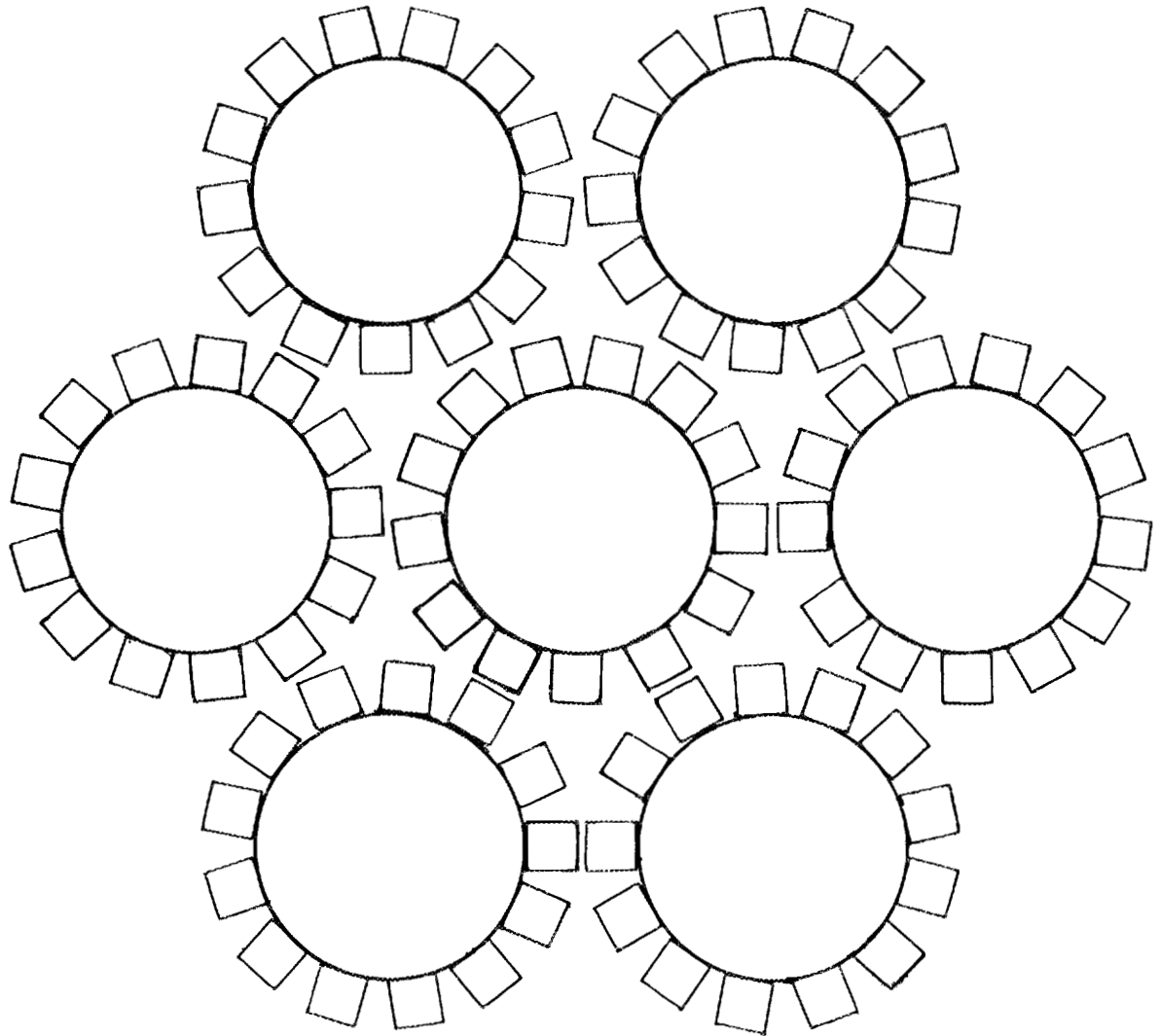


Fig. 12. Idealized Model of Air-Dried Carbon-Thoria Gel.

ORNL DWG 68-9432

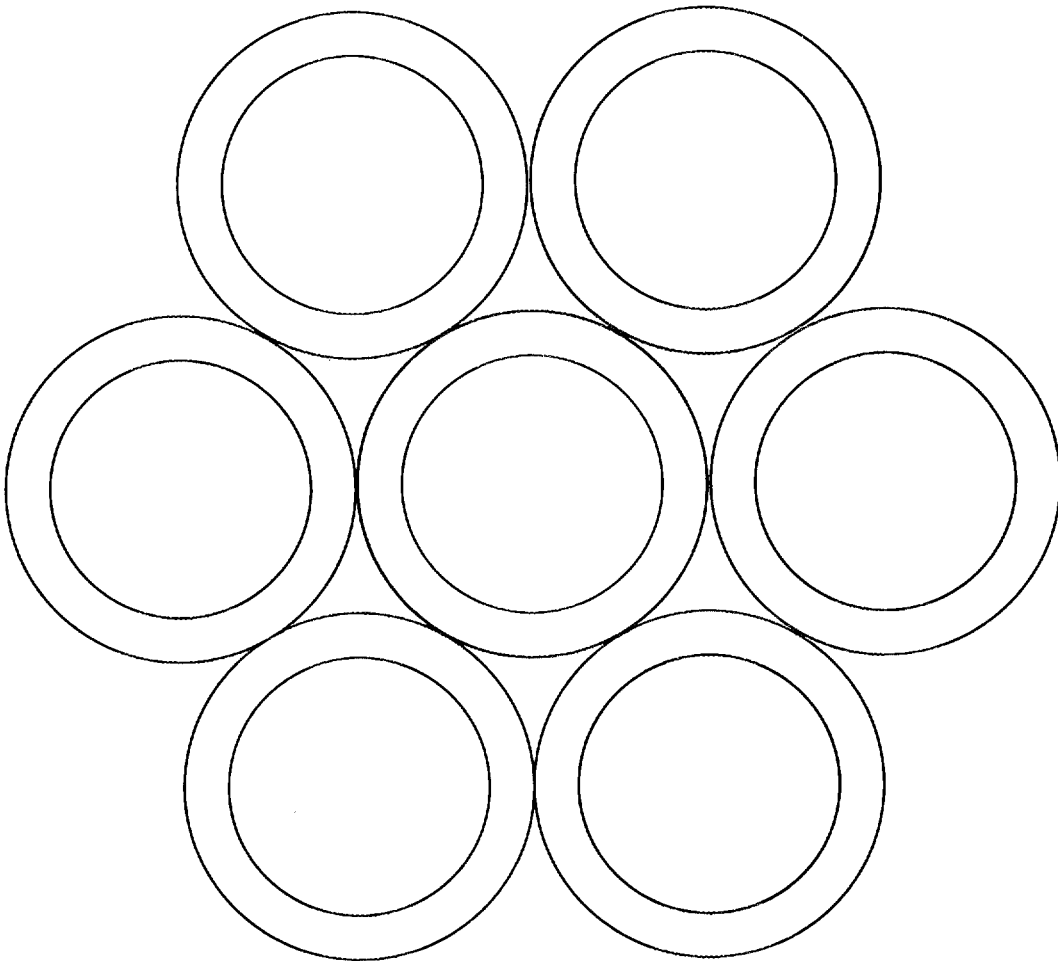


Fig. 13. Idealized Model of 1400°C-Sintered Carbon-Thoria Gel.

pores are known to be connected. Thus, the 50% factor between observed and calculated areas is in reasonable agreement with the above model. The pores themselves are probably larger than the measured size, since the measured value actually refers to the connecting openings through which the mercury must be forced.

Table 10. Surface Areas of Porous ThO₂

	Sample No.			
	III-133-1	III-134-1	III-133-3	III-134-3
C/ThO ₂ Mole Ratio	1	1	3	3
Porosity, %	14.5	13.0	45.2	47.0
Hg density at 1 atm	7.83	7.65	5.16	5.07
At 10,000 psi	9.16	8.80	9.41	9.57
Pore size range, A	170-250	170-350	190-440	170-440
Avg. pore size, A	200	190	320	320
Surface Area, m ² /g:				
Observed	2.5	2.5	8.0	8.1
Calculated	5.7	5.7	16.5	16.5

In many cases, the pore sizes are of about the same magnitude as the Spheron 9 particles, particularly in instances where the C/ThO₂ volume ratios are in the range 0.25 to 1.0 (i.e., at mole ratios of 1 to 4). At lower C/ThO₂ mole ratios, the pores are larger, perhaps because the thoria sinters away from the carbon particles. At higher mole ratios, it is probable that the carbon particles touch each other and create larger agglomerates and, in turn, larger pores. Therefore, in a porosity range of 15 to 60%, pore size control should be possible by using carbon blacks of larger or smaller particle size than Spheron 9. The lower size limit for commercially available material is about 100 A, while the upper limit for a readily dispersible carbon black is about 1000 A.

3.5 Residual Carbon

Prior to sintering, carbon was readily burned out of carbon-ThO₂ gels. However, if sintering preceded burning, the carbon was more difficult to burn out, particularly in the case of less porous gels (even though these contain a lower percentage of carbon). The problem became acute at porosities of about 3% or less (C/ThO₂ mole ratios ≤ 0.4). At C/ThO₂ ratios of 3 and higher, a period of 1 or 2 hr at 800°C in air was adequate to burn to a snow-white gel; at a ratio of 1.0, about 2 to 4 hr was required. At ratios of 0.4 and 0.1, as long as three days (at 800°C in air) was necessary to obtain a white oxide visually "free" of carbon. After a sample had passed the visual test, no special effort was made to reduce the carbon content further.

At C/ThO₂ mole ratios of 1.0 and 3.0, carbon analyzes of six products prepared by sintering at 1400°C and burning at 800°C were as follows:

Ratio of 1: 100, 140, 120 ppm

Ratio of 3: 300, 450, 380 ppm

All of these products were white and appeared to be homogeneous. The residual carbon from four other samples, having C/ThO₂ mole ratios of 0.1 and 0.4, were 360, 1700, 3400, and 2700 ppm. These products were not homogeneous; some fragments contained dark centers, indicating that oxygen diffusion was not yet complete.

At the higher porosities, diffusion was less of a problem, as indicated above. In connection with kinetic studies (Sect. 3.8), microspheres having a C/ThO₂ ratio of 4 were burned at about 500°C in air and at about 400°C in oxygen, each for approximately an hour. All products appeared homogeneous, and all were light blue-gray in color. Carbon analyses, in relation to the firing schedules, were as follows:

Burned in air at 460°C	2480 ppm
Burned in air at 480°C	2030 ppm
Burned in air at 500°C	2000 ppm
Burned in oxygen at 430°C	1640 ppm
Burned in oxygen at 450°C	1450 ppm

Since the burnout characteristics of gels with C/ThO₂ mole ratios of 0.1 and 0.4 are very different from those with ratios of 1.0 and higher, a gel having an intermediate C/ThO₂ ratio of 0.7 was prepared. Its burning properties classify it with the gels having C/ThO₂ ratios of 0.1 and 0.4. One explanation of the sharp line of demarcation between mole ratios of 0.7 and 1.0 can be stated as follows: At low C/ThO₂ ratios, the sintered thoria matrix completely surrounds and encapsulates each carbon particle; at higher ratios, the thoria matrix, although still continuous, is not present in sufficient volume to completely coat each carbon particle.

3.6 Graphite as Carbon Source

Five samples of porous thoria were prepared with graphite instead of Spheron 9 as part of the scheduled test program. Two C/ThO₂ mole ratios were used, and both standard firing schedules were used at each ratio. Results are summarized in Table 11, and are compared with the corresponding samples prepared with Spheron 9. The results for samples fired according to the sinter-burn firing schedule were as expected at a C/ThO₂ ratio of 3.0. The observed porosity agreed well with the calculated porosity (Fig. 7) (as in the case of the samples prepared with Spheron 9), and the pore size agreed with the BET (calculated) particle size of 0.2 μ. At a C/ThO₂ ratio of 0.4, the amount of porosity was greater than that obtained with samples containing Spheron 9 (but nearer the calculated value than was Spheron 9), whereas the pore size, although greater than at a C/ThO₂ ratio of 3.0, was still smaller than for samples containing Spheron 9. The porosities of the samples fired according to the burn-sinter cycle were low and, therefore, difficult to discuss. The two results for graphite samples appear to be anomalous, but it may be significant that, at the 3.4% level, the pore sizes are still in the 0.2-μ range.

One possible explanation for the poor results at low porosities is that the ThO₂ matrix is "squeezing out" porosity. The smaller pores introduced by Spheron 9 would be more mobile and, therefore, more likely to be "squeezed out;" they would also be more prone to coalesce into very large pores.

Table 11. Porous Thoria Prepared with Graphite

	Porosity (%)	Pore Size Distribution (% of total)			
		17-3 μ	3-0.5 μ	0.5-0.1 μ	1000-120 A
Sintered at 1400°C, burned at 800°C:					
C/ThO ₂ ratio = 0.4					
Graphite	6.8	26	64	7	3
Spheron 9	2.8	65	21	0	14
C/ThO ₂ ratio = 3.0					
Graphite	45.5	1	1	93	5
Graphite	46.6	0	0	95	5
Spheron 9	46.7	0	0	0	100
Burned at 800°C, sintered at 1400°C:					
C/ThO ₂ ratio = 0.4					
Graphite	3.4	9	8	74	8
Spheron 9	1.0	90	10	0	0
C/ThO ₂ ratio = 3.0					
Graphite	< 1	-	-	-	-
Spheron 9	2.0	-	-	-	-

3.7 Porous Microspheres

Table 12 gives results for several porous microspheres prepared by a sinter-burn firing schedule. The porosities are plotted vs the C/ThO₂ ratio in Fig. 14, and are compared with those of shards. The mercury porosity of the spheres follows a curve similar to that for the shards, except that the porosity of the spheres is about 10% greater. Part of the increased porosity is probably due to carbon acquired during sphere formation, which increases the C/ThO₂ mole ratio by about 0.2; this should add 1 to 5% porosity, depending on the original carbon content. The densities of spheres exhibit a far greater variation than those for shards. Five of the eight sphere samples have low densities in two instances, which indicate the presence of additional porosity.

The pore size distributions (Fig. 15) for spheres seem to follow a pattern in which the pore sizes are at a maximum at C/ThO₂ ratios of 3 to 4, then tend to become smaller at both higher and lower porosities. This trend differs from the distribution pattern for shards, in which the pore size increases monotonically with increasing porosity in the C/ThO₂ range of 1 to 6. Except at the highest porosity, the pore size at any given C/ThO₂ ratio is greater in spheres than in shards.

Post-sintering of III-115-2 spheres caused a smaller loss of porosity than for shards. For example, the original porosity of 64% decreased to 60% after sintering at 1200°C, and to 21% after sintering at 1300°C. (Compare with data in Table 8 for shards.) This greater resistance to sintering is due to the larger pore size of the spheres.

The differences between spheres and shards, with regard to porosity and pore size distribution, must result from differences in the gelation mechanism. One might speculate that, in the sphere forming column, rapid gelation "sets" the gel matrix in a looser structure, thereby increasing both pore size and total pore volume. This theory, however, does not agree with the results for samples III-55-C-1 and III-55-C-3, and III-55-D-1 and III-55-D-3 (Tables 4 and 5), in which neither rapid nor slow gelation caused significant effects. Consequently, it follows that either the spherical

Table 12. Data for Porous Microspheres

(Firing schedule: sintered at 1400°C, burned at 800°C)

Sample No.	C/ThO ₂ Mole Ratio	Porosity (%)	Pore Size Distribution (% total)							Density ^a
			17-3 μ	3-0.5 μ	0.5-0.1 μ	1000-580 A	580-350 A	350-250 A	250-120 A	
1-1-sphere	0.1	1.1	-	-	-	-	-	-	-	9.54
2-1-sphere	0.4	1.6	-	-	-	-	-	-	-	9.07
3-1-sphere	1.0	26	3	0	2	5	4	68	18	9.75
IV-12	3.3	51	0	0	0	0	81	13	6	7.93
III-115-4	4.0	63	0	0	0	0	80	15	5	9.04
III-115-2	4.1	64	0	0	3	90	7	0	0	8.03
IV-7	4.2	64	0	0	0	0	90	6	4	8.23
5-1-sphere	6.0	72	4	0	10	3	12	37	34	9.47

^aAt 10,000 psi.

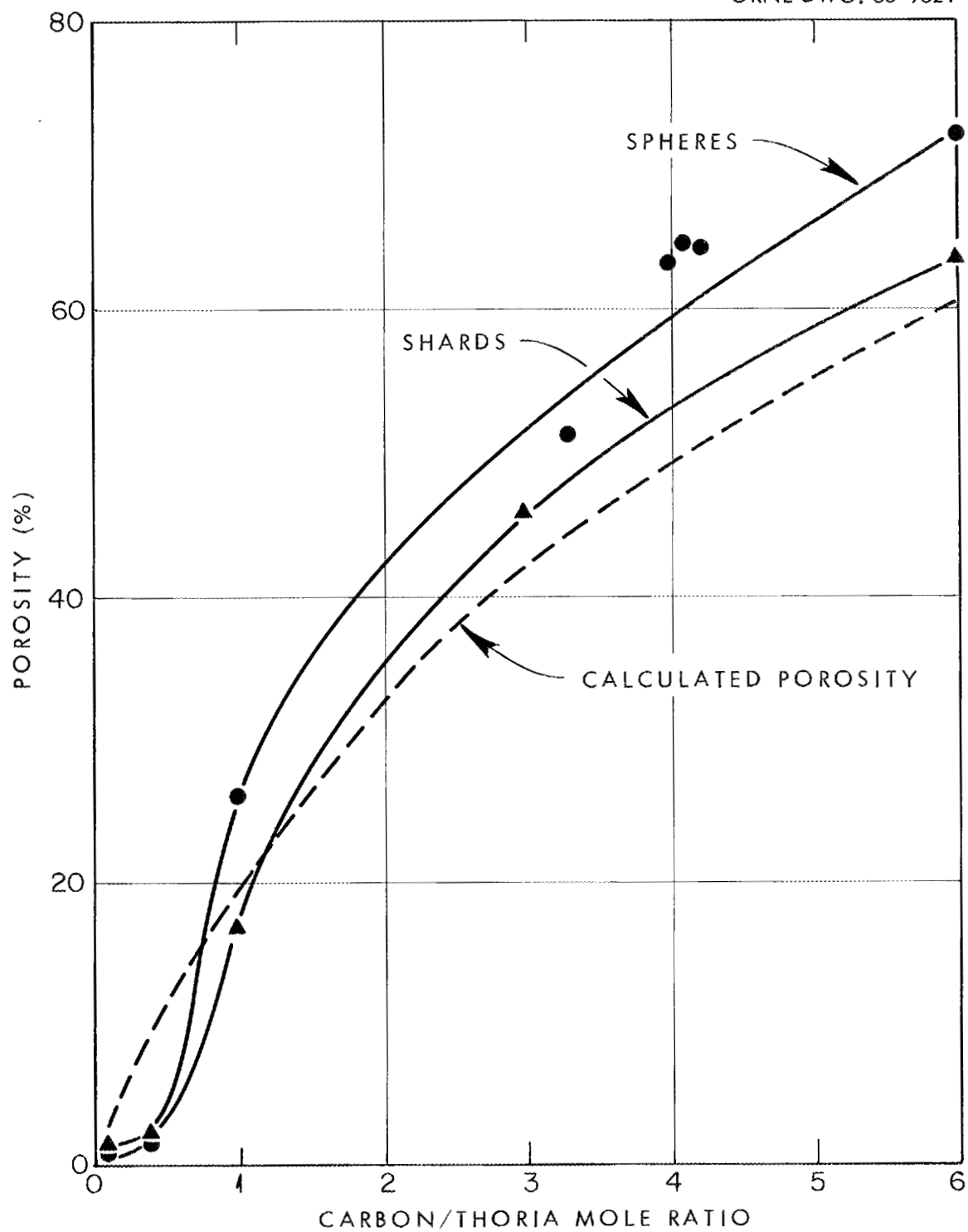


Fig. 14. Porosity of Microspheres as a Function of C/ThO₂ Mole Ratio of Sol. Calculated porosity curve and curve for shards shown for comparison.

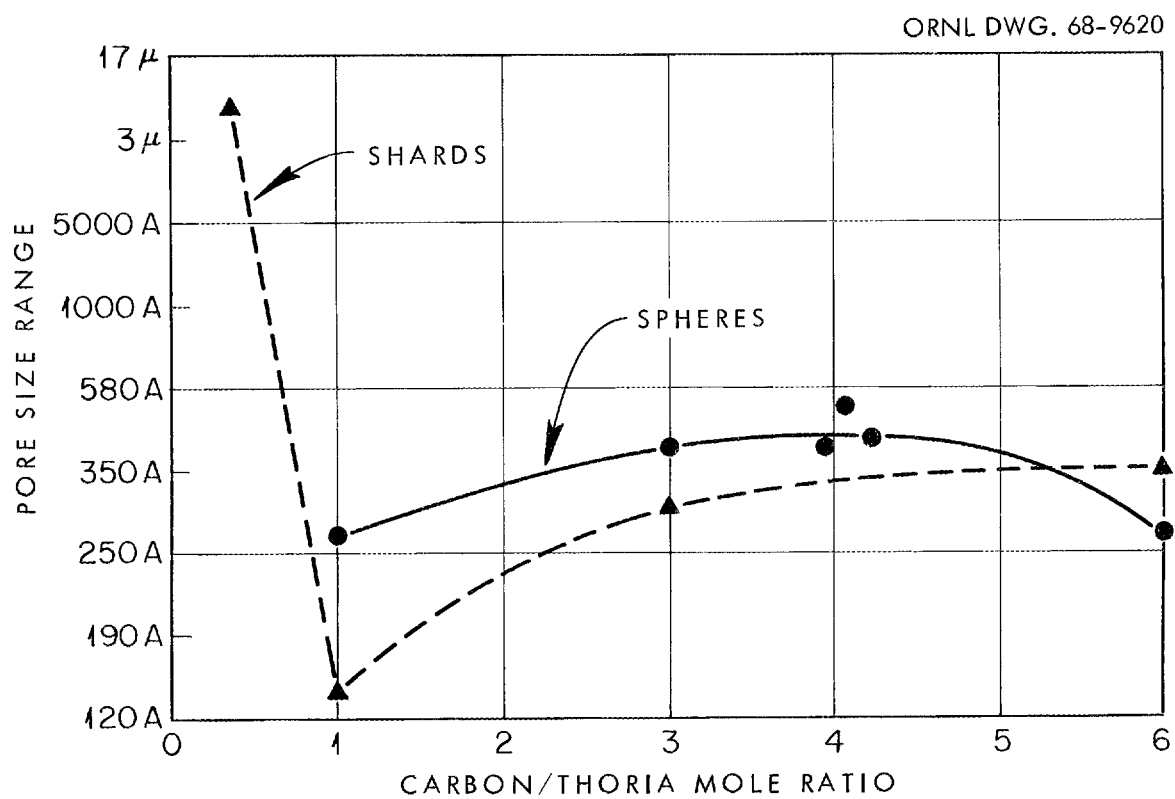


Fig. 15. Comparison of Pore Size Distributions of Shards and Spheres.

geometry or the presence of the solvent (and surfactants) cause microspheres to have somewhat different pore structure than shards.

The crushing strengths of spheres IV-7 and IV-12 were determined, with these results (data are the averages of four measurements each):

<u>Sample</u>	<u>Porosity, %</u>	<u>Sphere Diameter, μ</u>	<u>Avg. Crush Strength, g</u>
IV-7	64	500-530	150 \pm 30
IV-12	51	340-420	140 \pm 45

Four microsphere samples were prepared by using a burn-sinter firing cycle. These samples had low C/ThO₂ ratios (0.1 and 0.4), and each had a porosity of less than 1%.

3.8 Kinetics of Carbon Burnout

Carbon burnout kinetics were examined in order to obtain a better understanding of burnout rates in air, the temperature dependence of the burning rate, and the relative rates of carbon removal with oxygen and carbon dioxide. In connection with other work, carbon removal with hydrogen and steam was also tested. Kinetic studies were made on available microspheres, which contained 4.1 moles of carbon per mole of thoria and which had been presintered at 1000°C. These spheres had porosities of more than 50%, chiefly below 170 A in diameter; the mercury density at 10,000 psi (the cutoff point, corresponding to 170 A) was 2.71 g/cc.

Programmed temperature runs (rise rate, 400°C/hr) were conducted in various atmospheres, with the following results:

Air: Oxidation starts about 300°C, is rapid at 450°C, and is complete at 550°C.

Oxygen: Oxidation starts at 300°C, then becomes very rapid and goes to completion at 410°C.

Carbon Dioxide (Reaction $\text{CO}_2 + \text{C} \rightarrow 2\text{CO}$): Oxidation starts at 500°C, becomes rapid at 1000°C, and is completed at 1100°C.

Steam (Reaction: $\text{H}_2\text{O} + \text{C} \rightarrow \text{H}_2 + \text{CO}$): Oxidation starts at 850°C , becomes rapid at 925°C , and is completed at 1050°C .

Hydrogen (Reaction: $\text{C} + 2\text{H}_2 \rightarrow \text{CH}_4$): This reaction is discussed in the next section. It did not occur to a useful degree at temperatures up to 1000°C .

Oxidations in pure oxygen at 1-atm pressure could not be conducted under isothermal conditions. At temperatures of 430 and 440°C , self-heating of the sample (after admission of oxygen) caused an indicated 10 to 20°C rise in an adjacent thermocouple, and the reaction rate became very rapid.

In air, isothermal oxidations were conducted at 440 , 460 , 480 , and 500°C . These runs were made with whole spheres, at an air flow rate of 350 cc/min (STP). Two runs at 480°C were also made, one using powdered spheres and one at a gas flow rate twice that normally employed. The weight-vs-time curves were smooth, showing a short induction period of accelerating rate during the first 5% reaction, probably due to the time required to change over from argon to air atmospheres. After the inflection point, the rate decreased continuously, becoming asymptotic near completion. A typical curve, at 480°C , along with those for the two special runs at 480°C , is shown in Fig. 16.

The reaction rates in Fig. 16 are very similar, with the exception of the slightly faster rate for the run made at the higher flow rate. This indicates that the runs at the normal flow rate were slightly retarded by a deficient oxygen supply. (If any further work is to be done along this line, higher flow rates should be employed to completely eliminate this factor.) Since whole spheres reacted as fast as powdered spheres, the reaction rate is independent of the sample geometry. Therefore, the spheres are sufficiently porous to supply oxygen by diffusion as fast as it can be consumed chemically. This was further demonstrated by halting a reaction at a point halfway through the oxidation and withdrawing the partially reacted spheres. They were still black on the outside and, in cross section, appeared entirely uniform.

The rate data were fitted to various kinetic models, none of which was completely satisfactory for all the runs. The models tested were:

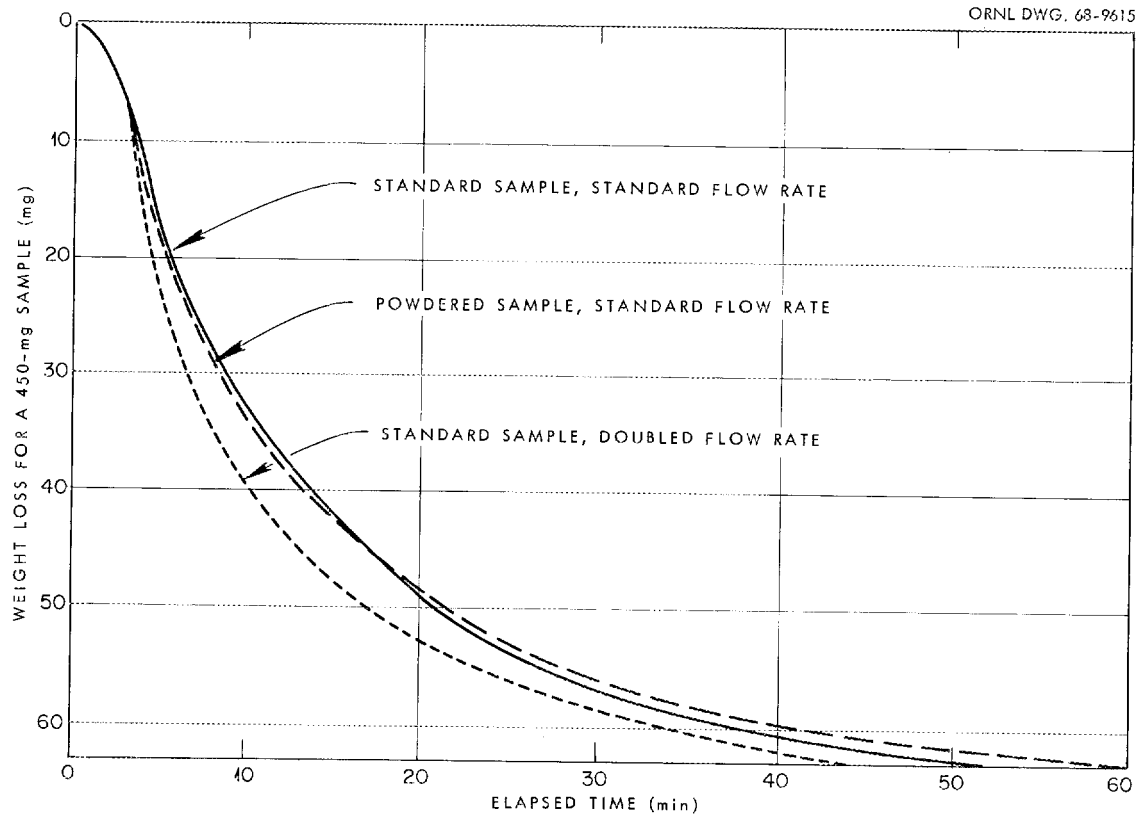


Fig. 16. Oxidation of C-ThO₂ Microspheres at 480°C in Air.

- (1) First order
- (2) Second order (in carbon)
- (3) Phase boundary (spherical model)
- (4) Phase boundary, plus diffusion control (spherical model)
- (5) First order, plus diffusion control.

The best overall fit, up to about 60% reaction, was provided by model (3). Even this model had rather large negative deviations at the higher temperatures. However, by using the first 60% of the data, reaction rates were obtained from the linear parts of the graphs. These values are listed below:

<u>Temperature, °C</u>	<u>Relative Rate</u>
502	38.1
479	20.9
460	9.7
439	4.3

These data were used to construct an Arrhenius plot (Fig. 17), which gave an activation energy of 40.9 kcal/mole. This value can be compared with results of Khaikina¹⁹ (40 kcal for electrode carbon, and 30 kcal for wood charcoal) and Patai *et al.*²⁰ (25 kcal for carbon black). The lower values for wood charcoal and carbon black may be the result of the presence of presorbed surface complexes of oxygen. These surface complexes are not present in electrode graphite, and have been largely driven off the carbon black in the present work by the 1000°C presintering treatment.

3.9 Porous (Th,U)O₂

One sample of porous ThO₂-UO₂ was prepared in order: (1) to demonstrate that the method for preparing porous ThO₂ can be extended to include mixed oxides, and (2) to compare the results with those for ThO₂. Spheron 9 carbon black was blended with a mixed Th(IV)-U(VI) oxide sol containing 22.0 cation % uranium; the C/metal mole ratio was 3.3. Gel shards were prefired at 1400°C under argon for 1 hr, and carbon burnout was then attempted in three ways:

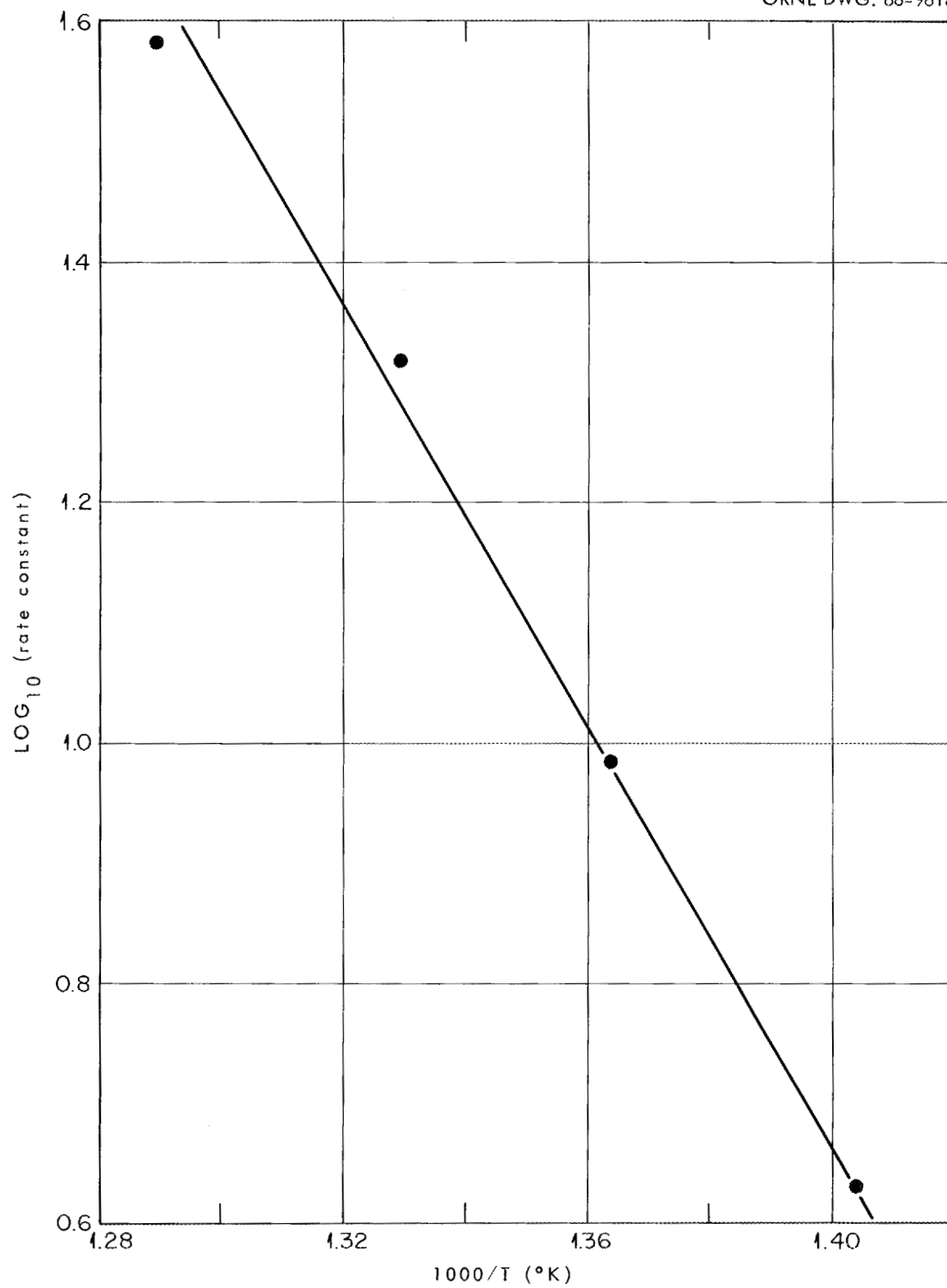


Fig. 17. Arrhenius Plot for Air Oxidation of Carbon.

- (1) in air at 800°C,
- (2) in air at 800°C, followed by H₂ at 1000°C,
- (3) in H₂ at 1000°C, using a slow temperature rise rate.

Both methods (1) and (2) were successful; the residual carbon contents were 50 and 180 ppm, respectively. Method (3), even though thermodynamically possible ($C + 2H_2 \rightarrow CH_4$), did not remove any significant amount of carbon (13.6% carbon in starting material vs 13.4% in product).

Products from methods (1) and (2) were identical. The porosity was 59%, higher than for ThO₂ at a comparable original carbon content (48%). Also, the pores were slightly larger, 440 to 870 Å vs about 400 Å for ThO₂.

X-ray diffraction (performed by R. L. Sherman, Analytical Division) of all three products and the sintered starting mixture showed only single-phase cubic structures. The product from method (2) gave the sharpest pattern, from which $a_o = 5.5705$ was determined, in agreement with the assumptions of ideal solid solution and the presence of uranium as U(IV). [From Vegard's Law and values of $a_o(UO_2) = 5.4682$ and $a_o(ThO_2) = 5.5997$, the calculated value for U_{0.22}Th_{0.78}O₂ is 5.5708.] The product from method (1) gave a slightly blurred pattern, probably because of the presence of interstitial oxygen. According to Anderson et al., this product should have been U_{0.22}Th_{0.78}O_{2.16}.

The final mercury density of products from methods (1) and (2) was 9.82, from which a closed porosity of 4% was calculated. These calculations were based on a theoretical density of 10.22, which was obtained by linear interpolation between the value for UO₂ and ThO₂. The value of 4% is about the same as the closed porosity (~5%) observed for porous ThO₂ in this porosity range.

4. SUMMARY AND CONCLUSIONS

A wide range of controlled porosity can be introduced into sol-gel thoria by incorporating carbon in the sol and subsequently burning the carbon out of the gelled shards or microspheres.

It has been demonstrated that any desired amount of porosity can be attained, up to a maximum of 72%. The degree of control is primarily a function of the precision with which the mixed carbon-thoria sols can be formulated.

The two primary variables are the carbon-thoria ratio and the sintering-burning method. For a firing schedule in which the thoria matrix is first "set" at 1200 to 1400°C, followed by carbon burnout at 800 to 1000°C, the porosity is about equal to the calculated volume of the carbon. However, if the operations in the firing schedule are reversed, much of the porosity introduced by carbon removal is sintered out. The temperature variations within these two general firing schedules are of lesser importance. However, porous thoria prepared by the first method will sinter if subsequently heated above 1200°C.

The pore size distribution is a function of the C/ThO₂ mole ratio, the firing schedule, the type of carbon used, and the type of material formed (gel shards or microspheres). Highly porous thoria with a narrow pore size distribution in the sub-micron range can be readily prepared. Thoria with pores in the micron range can also be prepared, but the porosity will be lower.

The carbon-thoria sols are very stable and are quite insensitive to operational variations during their preparation. The only variable in the gelation procedure found to have any effect on the porosity was whether shards or microspheres were formed. In general, the spheres had greater porosity and larger pore diameters than the corresponding shards.

The residual carbon contents of the porous oxides were relatively high (e.g., in the 190-450 ppm range). However, since no special effort has been made to obtain very low carbon contents, further work along these lines would probably lead to improvements.

The pore structure was related to the properties of the source carbon for both carbon black and graphite. Control over the pore size distribution should be possible, within limits, by proper selection of the carbon source.

A reasonable model of the gel structure and the sintering mechanics was constructed on the bases of porosity, pore size distribution, surface area, and density data. This model assumes a thoria matrix in which carbon is dispersed. The relative C/ThO₂ volume ratio determines the degree of openness of the final product.

The kinetics of carbon burnout in air was studied thermogravimetrically, and an activation energy of 41 kcal/mole was determined. Carbon removal by means of CO₂ and steam was demonstrated; hydrogen was not effective.

Porous mixed oxide of composition Th_{0.78}U_{0.22}O₂ with about 60% porosity was prepared. The product obtained was a solid solution of thoria-urania, which had a somewhat greater porosity than that found for ThO₂ prepared under similar conditions.

5. ACKNOWLEDGEMENTS

The availability of W. D. Bond for frequent discussions and free exchange of ideas is gratefully acknowledged. A. H. Mesch and C. K. Neulander, MIT Practice School, made major contributions, particularly in Sects. 3.1, 3.2, 3.3.1, 3.5, 3.6, and 3.7. Constructive comments were offered by K. H. McCorkle, S. M. Fleming, and S. T. Mayr. Chemical analyses were provided by W. R. Laing's group, Analytical Chemistry, with J. L. Botts performing most of the mercury porosity determinations.

6. REFERENCES

1. (a) A. D. Kelmers, ORNL, personal communication.
(b) W. Haller, "Chromatography on Glass of Controlled Pore Size," Nature 206, 693 (1965).
2. S. M. Fleming, MIT Practice School, and J. S. Johnson, ORNL, personal communication.
3. Chem. Technol. Div. Ann. Rept., May 31, 1965, ORNL-3830, pp. 174-176.
4. G. W. Horsley, L. A. Podo, and F. I. Wood, "Studies on the Reprocessing and Refabrication of HTGR Fuels in the OECD Dragon Project," Proceedings of the Conference on Fuel Cycles of High Temperature Gas-Cooled Reactors, Brussels (June 1965), EUR-2780e.
5. R. E. Leuze, ORNL, personal communication.
6. T. A. Gens, Preparation of Uranium and Thorium Oxide Microspheres with Controlled Porosity by a Sol-Gel Process, ORNL-TM-1530 (May 31, 1966).
7. Chem. Technol. Div. Ann. Progr. Rept, May 31, 1967, ORNL-4145, p. 206.
8. Fuel Cycle Studies Status Report for August, 1966, ORNL-CF-66-10-75, pp. 41-43.
9. A. H. Mesch and C. K. Neulander, Preparation of Thoria of Controlled Porosity, ORNL-MIT-3 (Oct. 14, 1966).
10. P. A. Haas and S. D. Clinton, Preparation of Thoria and Mixed Oxide Microspheres, ORNL-TM-1281 (November 1965).
11. D. E. Ferguson et al., Status and Progress Report for Thorium Fuel Cycle Development for Period Ending December 31, 1962, ORNL-3385, p. 33.
12. K. J. Notz, Mixed Sols of Carbon Black with Thoria and Other Oxides, ORNL-TM-1982 (in preparation).
13. P. A. Haas, S. D. Clinton, and A. T. Kleinsteuber, "Preparation of Urania and Urania-Zirconia Microspheres by a Sol-Gel Process," Can. J. Chem. Eng. 44, 348 (1966).

14. Fuel Cycle Studies Status Report for March, 1967, ORNL-CF-67-5-78, p. 15.
15. K. H. McCorkle, ORNL, personal communication.
16. D. E. Ferguson et al., Preparation and Fabrication of ThO₂ Fuels, ORNL-3225 (June 5, 1962), p. 15.
17. H. L. Ritter and L. C. Drake, "Pore Size Distribution in Porous Materials," Ind. Eng. Chem., Analyt. Ed. 17, 782 (1945).
18. S. Peterson, R. E. Adams, and D. A. Douglas, Jr., Properties of Thorium, Its Alloys, and Its Compounds, ORNL-TM-1144 (1965).
19. S. E. Khaikina, "Oxidation of Carbon," J. Tech. Phys. (USSR) 8, 53 (1938).
20. S. Patai, E. Hoffman, and L. Rajbenbach, "The Oxidation of Carbon by Air," J. Appl. Chem. 2, 306 (1952).
21. J. S. Anderson, D. N. Edgington, L. E. J. Roberts, and E. Wait, "The Oxides of Uranium. Part IV. The System UO₂-ThO₂-O," J. Chem. Soc. (London), 1954, 3324.

INTERNAL DISTRIBUTION

- 1-3. Central Research Library
- 4-5. ORNL - Y-12 Technical Library
Document Reference Section
- 6-10. Laboratory Records
11. Laboratory Records (RC)
12. ORNL Patent Office
13. Reactor Division Library
14. R. E. Adams
15. G. M. Adamson, Jr.
16. R. D. Baybarz
17. R. L. Beatty
18. J. E. Bigelow
19. R. E. Blanco
20. E. S. Bomar
21. W. D. Bond
22. B. S. Borie
23. G. E. Boyd
24. R. A. Bradley
25. R. E. Brooksbank
26. K. B. Brown
27. F. R. Bruce
28. S. R. Buxton
29. D. O. Campbell
30. J. M. Chandler
31. S. D. Clinton
32. C. F. Coleman
33. J. H. Coobs
34. F. L. Culler
35. J. E. Cunningham
36. F. L. Daley
37. D. E. Ferguson
38. L. M. Ferris
39. B. C. Finney
40. R. B. Fitts
41. J. H. Frye, Jr.
42. F. J. Furman
43. S. Fleming, MIT-ORNL
44. J. H. Gillette
45. A. T. Gresky
46. W. R. Grimes
47. P. A. Haas
48. R. G. Haire
49. J. P. Hammond
50. R. L. Hamner
51. W. O. Harms
52. C. C. Haws, Jr.
53. J. D. Hoeschele
54. A. R. Irvine
55. J. S. Johnson
56. F. A. Kappelmann
57. P. R. Kasten
58. A. D. Kelmers
59. F. J. Kitts
60. K. A. Kraus
61. N. A. Krohn
62. J. M. Leitnaker
63. R. E. Leuze
64. M. H. Lloyd
65. J. T. Long
66. A. L. Lotts
67. H. G. MacPherson
68. J. P. McBride
69. K. H. McCorkle
70. W. T. McDuffee
71. A. B. Meservey
72. J. G. Moore
73. L. E. Morse
74. E. L. Nicholson
75. R. Norman, GGA-ORNL
- 76-80. K. J. Notz
81. A. R. Olsen
82. J. R. Parrott
83. P. Patriarca
84. W. L. Pattison
85. W. H. Pechin
86. J. W. Prados
87. R. B. Pratt
88. A. D. Ryon
89. J. L. Scott
90. C. D. Sease
91. J. W. Snider
92. O. K. Tallent
93. E. H. Taylor
94. D. B. Trauger

INTERNAL DISTRIBUTION

- 95. W. E. Unger
- 96. V. C. A. Vaughen
- 97. T. N. Washburn
- 98. C. D. Watson
- 99. A. M. Weinberg
- 100. J. R. Weir, Jr.
- 101. M. E. Whatley
- 102. R. G. Wymer

EXTERNAL DISTRIBUTION

- 103. A. Amorosi, Argonne National Laboratory, LMFBR Program Office
- 104. J. E. Ayer, Argonne National Laboratory
- 105. R. H. Ball, RDT-OSR, P. O. Box 2325, San Diego, Calif. 92112
- 106. R. W. Barber, AEC, Washington
- 107. L. Burris, ANL, LMFBR Program Office
- 108. C. S. Caldwell, NUMEC, Apollo, Pa.
- 109. D. F. Cope, RDT, ORNL Senior Site Representative, AEC
- 110. G. W. Cunningham, AEC, Washington
- 111. C. B. Deering, RDT, ORNL Site Representative, AEC
- 112. W. Devine, Jr., Production Reactor Div., P. O. Box 550,
Richland, Washington 99352
- 113. E. W. Dewell, B&W, Lynchburg, Virginia
- 114. F. Forscher, Westinghouse, Penn Center Site, Pa.
- 115. M. L. Farrell, Atomic Energy Attache, Australian Embassy,
1700 Massachusetts Avenue, Washington, D.C.
- 116. A. Giambusso, RDT-AEC, Washington
- 117. A. J. Goodjohn, Gulf General Atomic, San Diego, Calif.
- 118. R. H. Graham, Gulf General Atomic, San Diego, Calif.
- 119. J. S. Griffo, AEC, Washington
- 120. N. Haberman, RDT-AEC, Washington
- 121. C. J. Hardy, AERE, Harwell, England
- 122. M. E. A. Hermans, KEMA, The Netherlands
- 123. P. G. Holstead, RDT-OSR, P. O. Box 550, Richland, Washington
- 124. S. Jaye, Gulf General Atomic, San Diego, Calif.
- 125. E. A. Kintner, Fuel Fabrication Branch, AEC, Washington
- 126. J. H. Kittel, Argonne National Laboratory, LMFBR Program Office
- 127. G. Kosiancic, Babcock & Wilcox, Lynchburg, Virginia
- 128. P. R. Landon, Lawrence Radiation Laboratory, Livermore, Calif.
- 129. W. J. Larkin, AEC-ORO

EXTERNAL DISTRIBUTION

130. S. Marshall, National Lead Company of Ohio
131. T. McIntosh, AEC, Washington
132. W. H. McVey, RDT-AEC, Washington
133. L. H. Meyer, Manager, Separations Chemistry Division,
Savannah River Laboratory
134. E. C. Moncrief, Babcock & Wilcox, Lynchburg, Virginia
135. R. L. Morgan, AEC-SROO
136. R. E. Pahler, RDT-AEC, Washington
137. C. W. Richards, AEC-Canoga Park
138. W. E. Roake, Battelle Northwest
139. H. M. Roth, AEC-ORO
140. J. W. Ruch, AEC-ORO
141. H. Schneider, AEC, Washington
142. H. Schumacher, EIR, Wuerenlingen, Switzerland
143. J. M. Simmons, RDT-AEC, Washington
144. E. E. Sinclair, AEC, Washington
145. K. G. Steyer, Gulf General Atomic
146. C. L. Storrs, HPO-AI/CE
147. J. A. Swartout, UCC, New York, N. Y.
148. L. V. Triggiani, W. R. Grace Research Div., Clarksville, Md.
149. C. A. Trilling, Atomics International
150. A. R. Van Dyken, Division of Research, AEC, Washington
151. A. Van Echo, RDT-AEC, Washington
152. R. P. Varnes, Combustion Engineering
153. W. R. Voigt, AEC, Washington
154. B. L. Vondra, NUMEC, Apollo, Pa.
155. M. J. Whitman, AEC, Washington
156. G. Wirths, Nuken, 645 Hanan, Postfach 869, West Germany
157. D. R. de Halas, Pacific Northwest Laboratory
- 158-173. Division of Technical Information Extension
174. Laboratory and University Division, AEC-ORO